Developmental Brain Research, 77 (1994) 227–250

BRES 51746

Maturation of the neuronal metabolic response to vibrissa stimulation in the developing whisker-to-barrel pathway of the mouse

Peter Melzer **, Egbert Welker *, Josef Dörfl, Hendrik Van der Loos

Institute of Anatomy, University of Lausanne, Rue du Bugnon 9, 1005 Lausanne, Switzerland

(Accepted 24 August 1993)

Key words: 2-Deoxyglucose autoradiography; Cytochrome oxidase; Mouse somatosensory system; Whisker stimulation; Barrel cortex; Somatotopy; Development of brain function

We examined functional maturation in the mouse whisker-to-barrel pathway from P2 (P0 is the day of birth) to adulthood using the autoradiographic deoxyglucose (DG) method. After intraperitoneal DG injection, left whiskers C1–3 and E1 were stimulated. Sections were cut transversely through the brainstem, and coronally or tangentially through the parietal cortex. After autoradiography, the sections were stained for Nissl or for cytochrome oxidase (CO) activity. In subnuclei caudalis and interpolaris of the spinal trigeminal nucleus ipsilateral to stimulation, DG uptake evoked by the deflection of whiskers C1–3 was present at P2; in subnucleus oralis, nucleus principalis and the contralateral nucleus ventrobasalis of the thalamus, at P4; and in the contralateral barrel cortex, at P7. The first stimulus-dependent DG uptake appeared a few days after the appearance of whisker-related patterns seen in the CO- or Nissl-stained sections. In subnuclei caudalis and interpolaris, areas of stimulus-dependent DG uptake were initially larger than the CO segments representing the stimulated whiskers. Later, areas of stimulus-dependent DG uptake and CO segments matched well. DG uptake evoked by the stimulation of whisker E1 appeared 2–3 days later than that evoked by stimulation of whiskers C1–3. In nucleus principalis, one large area of stimulus-dependent DG uptake covered the representations of the caudal whiskers of all five rows – an observation made at all ages studied. In thalamus, stimulus-dependent DG uptake was found laterally in nucleus ventrobasalis. In barrel cortex, at P7, stimulus-dependent DG uptake was restricted to layers III and IV, but covered more barrels than whiskers stimulated. At P9, a second spot of high DG uptake was seen in deep layer V in register with that in layers III and IV. From P10 onwards, stimulus-dependent DG uptake stretched from layer II to layer VI, and in layer IV, in which it was highest, it was restricted to the barrels C1–3 and E1. In all stations, stimulus-dependent DG uptake decreased in magnitude after P10. While the onset of stimulus-dependent DG uptake is the result of the establishment of functional projections up to that station, the subsequent changes in size of the responding areas may well be due to the partial elimination of terminals, the maturation of local inhibitory circuits, and/or the development of cortical projections to the nuclei of termination and to the thalamic relay.

INTRODUCTION

We here report on functional maturation in the mouse whisker-to-barrel pathway during postnatal development, studied with the autoradiographic deoxyglucose (DG) method[62]. Earlier, this technique has been used to study the functional development of two other sensory systems, also in rodents.

In the rat olfactory bulb, Astic and Saucier[3] observed that areas of increased DG uptake, evoked by exposure to odors, rose in number but shrank in size between the day of birth (P0) and P20 (notations of age based on different conventions have been converted to fit those we have adopted; see Material and Methods). The increase in the number of such areas coincided with the growth of axon terminals of first order olfactory neurons and with an increase in the number of glomeruli. The authors proposed that the shrinkage in size of areas was associated with the development of interglomerular inhibitory circuits and/or with the selective stabilization of synaptic connections between first and second order olfactory neurons.

In a study of the postnatal development of the gerbil auditory pathway, Ryan et al.[54], reported that DG uptake could be increased by stimulation with wide band noise in the cochlear nuclei at P11. At P13, stimulus-dependent DG uptake appeared, in addition, in the superior olivary complex and in the ventral

* Corresponding author. Fax: (41) (21) 3132925.
** Present address: Laboratory of Cerebral Metabolism, National Institutes of Mental Health, Bldg. 36, Room 1A05, Bethesda, MD 20892, USA.

SSDI 0165-3806(93)E0150-J

nucleus of the lateral lemniscus. At P15, it was seen in the dorsal nucleus of the lateral lemniscus, in the inferior colliculus and in the medial geniculate body, and finally, at P17, in the auditory cortex. Hence, in this pathway functional maturation proceeds from lower to higher stations.

In the trigeminal sensory system of mice and rats, the various stations possess whisker representations arranged in patterns homeomorphic with the pattern of the mystacial whiskers. In all stations but one, the subnucleus oralis of the spinal trigeminal nucleus, these representations are visible as segments of high succinyldehydrogenase (SDH) activity[5,20,34] and high cytochrome oxidase (CO) activity[4,37,38,76,80]. In two stations, nucleus ventrobasalis of thalamus (VB) and barrel cortex (BC), the representations can also be seen in Nissl-stained sections, respectively, as barreloids[64] and barrels[77]. Whisker representations have been described to be visible in Nissl-stained sections through Sc, Si and Np of the mouse[39,41] (but see Discussion). In subnuclei caudalis (Sc) and interpolaris (Si) of the spinal trigeminal nucleus, CO and SDH segments develop shortly before birth, while subnucleus oralis (So) never develops such segmentation[4]. In nucleus principalis (Np), the segmentation develops during the first three postnatal days[21], in VB on P2[5,20,80], and in BC on P4[20,34,53].

With the DG method, the postnatal maturation of responses to whisker deflection has been investigated only in BC of the rat by Kossut and Hand[36], who reported that the first response to the stimulation of one whisker occurs at P4. A distinct patch of stimulus-dependent DG uptake appeared in the cortical plate. At P8, a second focus of stimulus-dependent DG uptake appeared below the first one in deep layer V. Subsequently, the stimulus-dependent DG uptake filled the gap between the two foci, to finally extend towards pia and white matter. This 'metabolic column' was fully developed at P21 and remained throughout adulthood[36]. The authors did not document how they related the areas of increased DG uptake to the barrel whose whisker was stimulated.

Using the 'Lausanne whisker stimulator' (essentially a magnetic coil controlled by an electronic timer), a selected set of whiskers can be deflected at given repetition rates and amplitudes (but not in given directions) over any period of time. This manner of stimulation allowed us to demonstrate that stimulus-dependent DG uptake in barrel cortex was restricted to the barrel (or barrels) whose whisker (or whiskers) were deflected[43]. Moreover, we observed that stimulation of three adjacent whiskers in one row led to greater accumulation of DG in each individual whisker representation, than deflection of only one whisker. This held not only for the cortex but also for the nuclei of termination. Using the same stimulation paradigm we here report on a study aimed at answering the following questions: (i) when during postnatal development does glucose metabolism in the mouse somatosensory pathway start to reflect peripheral sensory stimulation?; (ii) how do the areas of stimulus-dependent DG uptake relate to the morphologically defined central representations of the stimulated periphery?; (iii) does the magnitude of the stimulus-dependent DG uptake change during postnatal development?

Preliminary reports of this work have appeared in abstract form[44,45,47].

MATERIALS AND METHODS

Animals

Nearly 'à terme' pregnant albino mice of different lines bred from ICR-stock[65], were checked every day at 08.00 h. The 24 h period following the detection of a litter was called postnatal day 0 (P0). As a consequence, a given animal may have been as much as 24 h older than its assigned age. Whisker patterns of the newborn animals were recorded and the litters reduced to about eight animals. We only studied animals with whisker patterns that were close to standard; notably, animals with supernumerary follicles between rows B and C were not used[65]. Infant mice from both sexes were used, their age ranging from P2 to P18. Mice older than 6 weeks were taken as adults.

Preparation of mice and stimulation of whisker follicles

Mice from P2 to P13 were separated from their mothers about 15 h prior to stimulation to reduce their plasma glucose concentration; they were kept in a cage at room temperature without access to food and water, neither before nor during stimulation. About 30 min before stimulation, they were immobilized with gauze and adhesive tape. Without anesthesia, pieces of mu-metal wire, 1.0 (animals at P2) or 1.5 mm long (P4–P13) and 0.2 mm in diameter, were glued onto left whiskers C1, C2, C3, and E1 about 2 mm above the skin; all other whiskers on both sides were clipped.

Mice at P18 and adult animals were anesthetized with Nembutal (sodium pentobarbital, i.p. 60 mg/kg b.wt.) at least 15 h prior to stimulation. Pieces of mu-metal wire, 1.5 mm long and 0.2 mm in diameter, were glued onto left whiskers C1–3 and E1 about 2 mm (for P18) or 5 mm (for adults) above the skin and all other whiskers on both sides were clipped. The mice were restrained on polystyrene foam casts with adhesive tape. This procedure did not seem to upset the animals; it rendered them incapable of removing the metal pieces. Total time that animals were under anesthesia was about 45 min. Until stimulation, the animals were deprived of food but not of water, and during stimulation they were deprived of water as well.

The mice were injected intraperitoneally with [1-^{14}C]2-deoxy-D-glucose (DG) in saline (New England Nuclear, DuPont de Nemours and Co., Wilmington, DE, USA; 16.5 μCi/100 g b.wt.; 100 μCi/100 μl) and immediately afterwards exposed to magnetic field bursts for 45 min. The design of the magnetic stimulator is such that the magnetic field strength is the same in any horizontal plane, while it changes little in the vertical plane near the center of the coil. Since animals were restrained head movements were limited, and therefore did not cause the impact of the magnetic field on the metal pieces to differ much between animals and, in one animal, between rows of whiskers. For further details of the stimulation procedure see ref. 43. Table I summarizes the experiments. Stimulus parameters are detailed in Table II. At all ages, we applied a 'routine' stimulation consisting of magnetic field bursts with a repetition rate of 7.4

TABLE I

Summary of the experiments

Column 1: numbers give the sequence in which the experiments were carried out; animals marked with asterisk were subjected to non-routine stimuli which are defined in Table II. Column 2: age is given in postnatal days (P; birth is at P0). Column 3: body weight of the mice in grams at the moment of the DG experiment. Column 4: magnetic field strength applied during stimulation; 'H' = high strength, 'L' = low strength, 'S' = super strength used with M96 (see Table II for details). Column 5: '+' indicates that the animal was perfused; '−', that it was not. Column 6: 'C' means that the prosencephalon was cut coronally and brainstem and spinal cord were cut transversely; 'T', that the hemisphere was cut tangentially to the pial surface over the barrelfield. 'T,C' means that the barrel cortex was cut tangentially and the brainstem and spinal cord transversely. Column 7: 'N' (Nissl) means that sections were stained with Cresylecht violet; 'CO' that, in an alternate series, sections were stained for cytochrome oxidase activity. Column 8: '+' indicates that there was stimulus-dependent DG uptake in Sc, Si, So, Np, VB, and/or BC; '−', that there was not (blanks indicate that the region in question could not be analyzed). In this table we do not distinguish between DG uptake at the representations of whisker follicles C1–3 and follicle E1. Column 9: '+' marks the experiments in which optical densities (ODs) were measured to demonstrate changes in the stimulus-dependent DG uptake in Si, VB and BC (see Fig. 11). Column 10: list of figures in which photographic material from a given experiment was used.

(1)	*(2)*	*(3)*	*(4)*	*(5)*	*(6)*	*(7)*	*(8)*						*(9)*	*(10)*
Code	*Age (P)*	*Body weight (g)*	*Magnetic field strength*	*Perfused*	*Cutting plane(s)*	*Stained for*	*Stimulus-evoked DG uptake*						*OD*	*Figures*
							ipsilateral				*contralateral*			
							Sc	*Si*	*So*	*Np*	*VB*	*BC*		
M74	P 2	1.9	H	+	C	N, CO	−	−	−	−	−	−		
M75	P 2	1.9	H	+	C	N, CO	+	+	−	−	−	−		2,3,6,7
M92	P 2	2.1	H	+	C	N, CO	+	−	−	−	−	−		
M48	P 4	2.6	L	+	C	N, CO	+	+	−	−	+	−	+	1,2
M70	P 4	2.7	L	+	C	N, CO	+	−	−	−	−	−		
M40	P 4	3.0	H	+	C	N	+	+	−	−	+	−		
M41	P 4	3.1	H	+	C	N, CO	+	+	+	+	+	−		6,7
M72	P 4	3.1	H	+	C	N, CO	+	+	+	+	+	−		3
M73	P 4	3.0	H	+	C	N, CO	+	+	−	−	−	−		
M76 *	P 4	2.9	H	+	C	N, CO	+	+	+	+	+	−		4
M95 *	P 4	2.8	H	+	C	N	+	+	+	+	−	−		
M97 *	P 4	3.3	H	+	C	N	+	+	+	+	+	−		4
M96 *	P 4	3.0	S	+	C	N	+	+	+	+	+	−		
M17	P 4/5	3.4	L	+	C	N, CO			−	−	−	−		
M20	P 5	2.9	L	+	C	N, CO	+	+	−	−	+	−		
M66	P 6	4.5	L	+	T	N						−		
M67	P 6	4.2	L	+	T	N						−		
M68	P 6	4.5	L	+	T	N						−		
M69	P 6	4.2	L	+	C	N, CO	+	+	−	−	+	−	+	
M21	P 7	5.2	L	+	C	N			−	−	+	−		
M22	P 7	5.4	L	+	C	N			−	−	+			
M35	P 7	5.4	L	+	C	N, CO		+	+	+	+	+	+	1,8
M36	P 7	6.0	L	+	C	N, CO					+	+	+	
M37	P 7	5.8	L	−	C	N, CO					+	+	+	
M77	P 7	6.0	L	−	C	N, CO	+	+	+	+	+	−	+	
M78	P 7	5.8	L	+	T	N						−		
M89	P 7	4.7	H	+	T, C	N, CO	+	+				−		
M90	P 7	3.2	H	+	T, C	N, CO	+	+				+		9
M27	P 9	5.0	L	+	C	N, CO		+	+	+	+	+	+	
M28	P 9	5.6	L	+	C	N, CO		+	+	+	+	+	+	7
M29	P 9	5.6	L	+	C	N, CO		+	+	+	+	+	+	
M30	P 10	6.0	L	+	T	N						+	+	
M31	P 10	5.6	L	+	T	N						+	+	9
M32	P 10	5.8	L	−	C	N, CO		+	−	−	+	+	+	1
M71	P 10	6.0	L	+	C	N, CO	+	+	+	+	+	+	+	2,3,5,6
M23	P 11	7.5	L	+	C	N, CO		+	+	+	+	+	+	
M24	P 11	7.4	L	+	C	N, CO		+	+	+	+	+	+	
M98	P 13	8.8	L	+	C	N, CO	+	+	−	+	−	+	+	
M99	P 13	9.4	L	+	C	N, CO	+	+	+	+	+		+	1
M100	P 13	9.1	L	+	C	N, CO	+	+	+	+	+	+	+	
M101	P 18	7.9	L	+	C	N, CO	+	+	−	+	−	+	+	
M102	P 18	7.8	L	+	C	N, CO	+	+	−	+	−	+	+	6
M103	P 18	7.7	L	+	C	N, CO	+	+	−	+	−	+	+	2,3
M141	P 45	26.6	L	+	T, C	N						+	+	
M42	P 60	28.0	H	+	T	N						+		9
M43	P 60	26.0	H	+	C	N	+	+	+	+	−	+		
M18	P 69	33.5	L	+	C	N		+	+	+	−	+	+	1

s^{-1}. The bursts contained the 50 Hz alternating current of the mains. As part of routine stimulation, a low and, in several experiments at P2, P4, P7 and P60, a high magnetic field strength were used (see Table II). In one experiment at P4 (M76), the magnetic field bursts as well as the interburst pauses were lengthened and the period of stimulation was increased, while in three other experiments with P4 mice (M95, 96, 97), bursts were delivered in trains (Table II).

Tissue processing and histology

Immediately after the 45 min of stimulation, animals were anesthetized with Nembutal and perfused through the heart with 3.3% formalin in 0.1 M Sörensen-buffer (pH 7.4) for 10 min[10]. Upon perfusion, the brains, including the two upper cervical segments of the spinal cord, were dissected out. Three mice were not perfused (Table I); their brains were removed immediately and processed as the others.

For coronal sections, the brains were placed on Teflon trays so that the cerebral hemispheres and the brainstem were in one longitudinal axis. Thus, transverse sections through the brainstems were in the same plane as the coronal sections through the hemispheres. In order to obtain sections cut tangential to the pial surface above BC, the brain was divided in the mid-sagittal plane and the hemispheres were further trimmed to obtain the appropriate angle for tangential cutting using a miniature guillotine[52], and placed on a plastic holder. Following this procedure it was impossible to collect sections through VB from these hemispheres. In three experiments, the brainstem had been separated before the hemispheres were divided. These brainstems were cut transversely and the hemispheres cut tangentially (cases 'TC' in column 6, Table I).

Subsequently, all specimens were frozen in dry-ice-chilled isopentane, and mounted on an object holder with cooled M-1 embedding matrix (Lipshaw, Detroit, MI 48210, USA). Sections were cut at 20 μm in a cryostat at −16°C (Frigocut 2700, Reichert-Jung, Nussloch, Germany). The sections were collected on chrome alum-coated slides. From most of the coronally cut brains, two alternate series of sections were collected. One series was dried on a hot plate at 60°C, whereas the other series was thaw-mounted and freeze-dried overnight at −18°C.

Both series of sections were exposed to Cronex MRF 31 film (Du Pont de Nemours and Co., Wilmington, DE, USA) with the vacuum-contact-method[35] at 5°C for 2 weeks. The sections were co-exposed with calibrated radioactivity sources. These sources were prepared[15] and calibrated for equivalent radioactivity content in brain tissue (nCi/g) using a series of poly[^{14}C]metamethacrylate reference sources (set no. C 791, Amersham, Amersham, UK). After development of the film[43], the hot plate-dried sections were stained with Cresylecht violet, whereas the freeze-dried sections were stained for CO activity[43,75].

Qualitative assessment of the autoradiograms

The autoradiograms were inspected for localized stimulus-dependent DG uptake (Table I). We have analyzed DG uptake in Sc, Si, So, Np, VB and BC. Uptake was considered stimulus-dependent when the opposite side was available for comparison and showed no such uptake. Referring to the amount of local DG accumulation we use the term 'magnitude'.

From each mouse with stimulus-dependent DG uptake in one or more stations of the pathway, some sections were selected to study the correspondence between the focus, or foci, of DG uptake and the representations of the stimulated whiskers as seen in the CO- or Nissl-stained preparations.

Using a light microscope fitted with a drawing tube, the perimeters of the sections as well as those of barrels were drawn from Nissl-stained tangential sections through BC. Outlines of CO segments were drawn from coronal sections through BC and VB, and from transverse sections through Np, Si and Sc. The drawings were used as anatomical reference for areas of DG uptake by superimposing them on photographic enlargements of the corresponding autoradiograms. For photographic prints we routinely used relatively hard paper (numbers 3 and 4). In order to obtain prints of adequate contrast, it was found to be advantageous to slightly underexpose. For the topological correspondence between CO segments and whisker follicles, see Discussion.

Densitometry of autoradiograms

In order to compare quantitatively stimulus-dependent DG uptake among mice, we selected animals which had been exposed to routine stimulation of low strength (Table I, column 9). Transmittance of light in and near areas of stimulus-dependent DG uptake was measured on digitized images of autoradiograms with a TV camera-based image analysis system (ASBA, Wild and Leitz, Zürich, Switzerland). These areas were outlined by the observer on the system's video display. The system calculates the mean transmittance of light from all pixels in the outlined area (one such area contained from about 15 to about 400 pixels). From these means, mean optical densities (mODs) were determined. mOD was defined as the logarithm of the ratio between the mean transmittance of light in an area of 'bare' film near the autoradiogram and the mean transmittance of light determined in the area of interest in the autoradiogram.

mODs were determined for: (i) the areas with a stimulus-dependent increase in DG uptake in a given station and (ii) an immediately neighboring area in that station up to the station's approximate boundaries, representing 'non-activated' tissue. We took the ratio (R) of the mODs of (i) and (ii) as an index for the magnitude of the stimulus-dependent DG uptake. In VB, we tested whether the ratio of activation would change, when mODs from the homotopic area on the 'non-stimulated' side were taken as denominator. The ratios

TABLE II

Summary of routine and of unconventional parameters of stimulation applied to follicles of left whiskers C1–3 and E1

Upper two rows: low and high field strength routine stimulation as used in the majority of experiments (see Table I). In the lower rows, the stimulus parameters of four P4 animals are presented (column 1 gives their codes; same animals as those marked with an asterisk in Table I, column 1). In columns 3 and 4, '−' signifies that bursts with a continuous repetition rate were used instead of trains of bursts. Column 8 gives the sum of all burst durations during the time of stimulation ('T_{on}'). In column 9 the power 'P', and in column 10 the energy ('$P \times T_{on}$') to which the mice were exposed are given.

(1)	*(2) Strength of magnetic field (10^3 A/m,rms)*	*(3) Duration of burst trains (ms)*	*(4) Duration of intertrain pauses (ms)*	*(5) Burst duration (ms)*	*(6) Pause duration (ms)*	*(6) Repitition rate (s^{-1})*	*(7) Period of stimulation (min)*	*(8) T_{on} (min)*	*(9) Power P (W)*	*(10) Energy $P \times T_{on}$ (10^4 Ws)*
Routine, low	6.1–7.2	–	–	46	90	7.4	45	15.3	16.9	1.6
Routine, high	9.2–10.2	–	–	46	90	7.4	45	15.3	36.2	3.3
M76	10.1	–	–	150	300	2.2	90	30.0	36.2	6.5
M95	10.1	490	510	46	24	7.0	45	14.5	36.2	3.1
M97	10.1	1400	1400	46	24	7.1	45	14.8	36.2	3.2
M96	14.3	700	1400	46	54	3.3	45	6.8	74.6	3.1

were not significantly different from those calculated using mODs of non-activated tissue adjacent to activated area. We opted for the latter approach, if only to avoid the consequences of occasional deviations from the coronal plane of section.

Quantification was performed in Si, VB and BC. In Si, activated and non-activated areas were measured ipsilateral to stimulation; in VB and BC, contralateral to stimulation. In Si and VB, autoradiograms of transverse (= coronal) sections were used. In BC, activated and non-activated areas were measured in layer IV; measurements were made from autoradiograms of coronal and tangential sections, and the data were pooled. If in Si, and in tangentially cut BC, areas of DG uptake evoked by stimulation of whiskers C1–3 and E1 could be distinguished, they were measured separately. Per animal, readings were collected from as many autoradiograms from a given station as possible. No measurements were made when the areas of interest showed even small destruction of the tissue.

Statistical analysis of densitometry

Using a statistical analysis package[56], the results were submitted to the following procedures: (i) linear regressions were calculated between the mOD of all measured areas as dependent variable, and radioactivity content as the independent variable; (ii) since for an individual mouse the distribution of Rs from a given station was never normal, the median of the ratios was taken to represent the Rs of Si, VB and BC. These medians were subjected to a non-parametric analysis of variance using the Wilcoxon/Kruskal–Wallis test. In this analysis, the medians of R for a given area were compared among ages. For those sets of data for which the Wilcoxon/Kruskal–Wallis tests detected significance at $P \leq 0.05$, a Tukey's studentized range test was performed on ranks so as to determine which groups were significantly ($P \leq 0.05$) different. The non-parametric analysis does not allow multiple statistical comparison between observations made in the same subject. This holds in our case for the comparison at a given age between values from C1–3 and E1 within a station, and between values from different stations.

RESULTS

Qualitative description

The overall DG uptake in the brains of mice at P7 and younger varied considerably and independently from age. Seven mice had a low, uniform tracer distribution, patternless to the point that neither stimulus-dependent DG uptake nor the boundaries between gray and white matter could be discerned. These mice were excluded from further analysis. Apparently, a threshold amount of DG must accumulate in brain tissue to reveal metabolic patterns in general, and stimulus-dependent changes in neural metabolism in particular. The whisker stimulation as used in this study could not be carried out on mice younger than P2, since the whiskers of these mice were too weak to support the pieces of metal.

The mice analyzed are listed in Table I, where we recorded the presence or absence of stimulus-dependent DG uptake in the nuclei of termination (Sc, Si, So and Np) ipsilateral to stimulation as well as in VB and BC, both contralateral to stimulation. Fig. 1 provides an overview of the appearance of stimulus-dependent DG uptake in brainstem, thalamus and cortex in five selected ages. The size of the areas of stimulus-dependent DG uptake is typical for each age. It seemed independent from field strength of the stimulus, as shown by experiments with mice at P4 (where three field strengths were used) and at P7 and with adults (two field strengths). In the description below, emphasis is given to cases in which stimulus-dependent DG uptake is present, and to ages at which new aspects of stimulus-dependent DG uptake appear in development.

The brainstem nuclei (Figs. 1 to 6)

At P2, three mice were stimulated with high strength routine stimulation (Table II). A whisker map of CO segments was visible in Sc, Si and Np. In two mice, stimulus-dependent DG uptake in Sc was found in a single area at its medial boundary. The area covered CO segments of row C and spread into neighboring rows (Fig. 2). In one of these mice, a single area of stimulus-dependent DG uptake stretched over a number of central CO segments in Si, including those of row C, at the lateral boundary of the subnucleus (Fig. 3). In So and Np (Fig. 6), stimulus-dependent DG uptake was not observed.

At P4, a total of 10 animals was analyzed. Six had been subjected to routine stimulation with either high or low strength (Table II). Their Sc showed an area of stimulus-dependent DG uptake covering the medial CO segments of row C and neighboring rows (Fig. 2). In Si, in five of the six mice, one area of stimulus-dependent DG uptake was found at the lateralmost segments of row C and, again, it spread into neighboring rows (Fig. 3). With low and high strength routine stimulation, the number of CO segments with stimulus-dependent DG uptake was about equal. Stimulation of the four mice with stimuli other than routine (Table II) resulted in areas of stimulus-dependent DG uptake in Sc and Si comparable to those described above (M97 in Fig. 4). In one of these four mice (M76), an additional small area of increased DG uptake was observed in row E, medial in Sc and lateral in Si (Fig. 4). The magnitude of DG uptake of this area was smaller than that of the DG uptake related to the stimulation of whiskers C1–3. This animal was stimulated for 90 min at a repetition rate considerably lower than that of routine stimulation. Of the 10 mice, 6 had stimulus-dependent DG uptake in So and Np. In So, one large area of stimulus-dependent DG uptake could be discerned in the center of the nucleus close to its lateral boundary. In Np, one large area spanned the entire ventral border (Fig. 6).

At P7, with low and high strength stimulation, in Sc and Si one large area of stimulus-dependent DG uptake was centered over, but was larger than, CO seg-

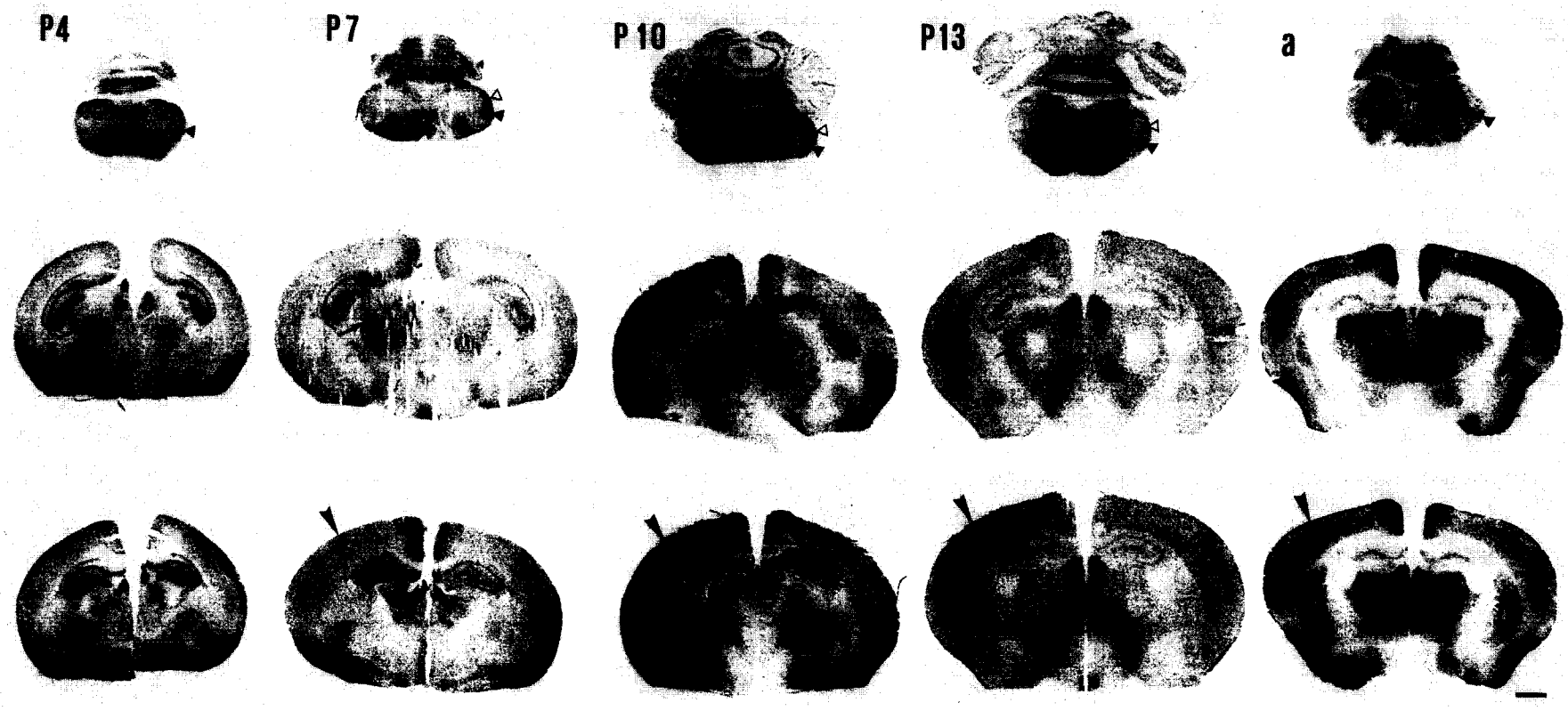

Fig. 1. Autoradiograms of 20 μm thick sections through subnucleus interpolaris (top row of panels), nucleus ventrobasalis of the thalamus (center row) and barrel cortex (bottom row) of mice at postnatal days (P) 4, 7, 10, 13 and 69 (adult, a). Sections were cut transversely (= coronally) through brainstem and brain. In each column, autoradiograms of the same animal are displayed. Follicles of left whiskers C1–3 and E1 were stimulated using low strength routine stimulation (Table II). At all ages, in the left subnucleus interpolaris there is one large area of high DG uptake (solid triangles) related to the stimulation of the three whiskers in row C. An additional small area of less increased DG uptake (open triangles), related to the stimulation of whisker E1, is present from P7 to P13. From P4 to P13, there is an area of stimulus-dependent DG uptake in the contralateral nucleus ventrobasalis of the thalamus (arrows). In the right barrel cortex, stimulus-dependent DG uptake becomes visible at P7 (arrowhead). With progressing age, neural activity is transmitted from brainstem to cortex and radiates from layer IV (where its magnitude remains highest) into layers II and VI. Orientation: dorsal is up; the animal's left is to the right. Bar at lower right represents 1 mm and holds for all panels.

ments in row C. A second, smaller area of stimulus-dependent DG uptake was located more dorsally in these subnuclei (as shown for Si in Fig. 1, top row). This held for all animals in which these subnuclei could be studied. Stimulation at high strength did not result in patterns of DG uptake different from those evoked by stimulation at low strength. In four animals, So and Np lent themselves to analysis; in two of them a single large area of stimulus-dependent DG uptake was present in the middle of the nuclei close to their respective lateral and ventral borders.

At P10, in Sc a large area of stimulus-dependent DG uptake was present near its medial border in the one animal in which this subnucleus was available for study. The highest DG uptake was centered over the CO segments of row C, with spread over segments of adjacent rows (Fig. 2). In Si of the two animals analyzed, two separate areas of stimulus-dependent DG uptake were present near its lateral border. One area was in the middle of the subnucleus; another was more dorsal (Fig. 3). In one mouse we found a single area of stimulus-dependent DG uptake covering a large part of So (Fig. 5) and of Np (Fig. 6).

At P13, in the three animals studied, in Sc one large area of stimulus-dependent DG uptake was limited to three CO segments in row C at the medial border of the subnucleus. A second area of stimulus-dependent DG uptake was clearly separated from it and was restricted to one medial CO segment in row E. In Si, again in all three mice analyzed, stimulus-dependent

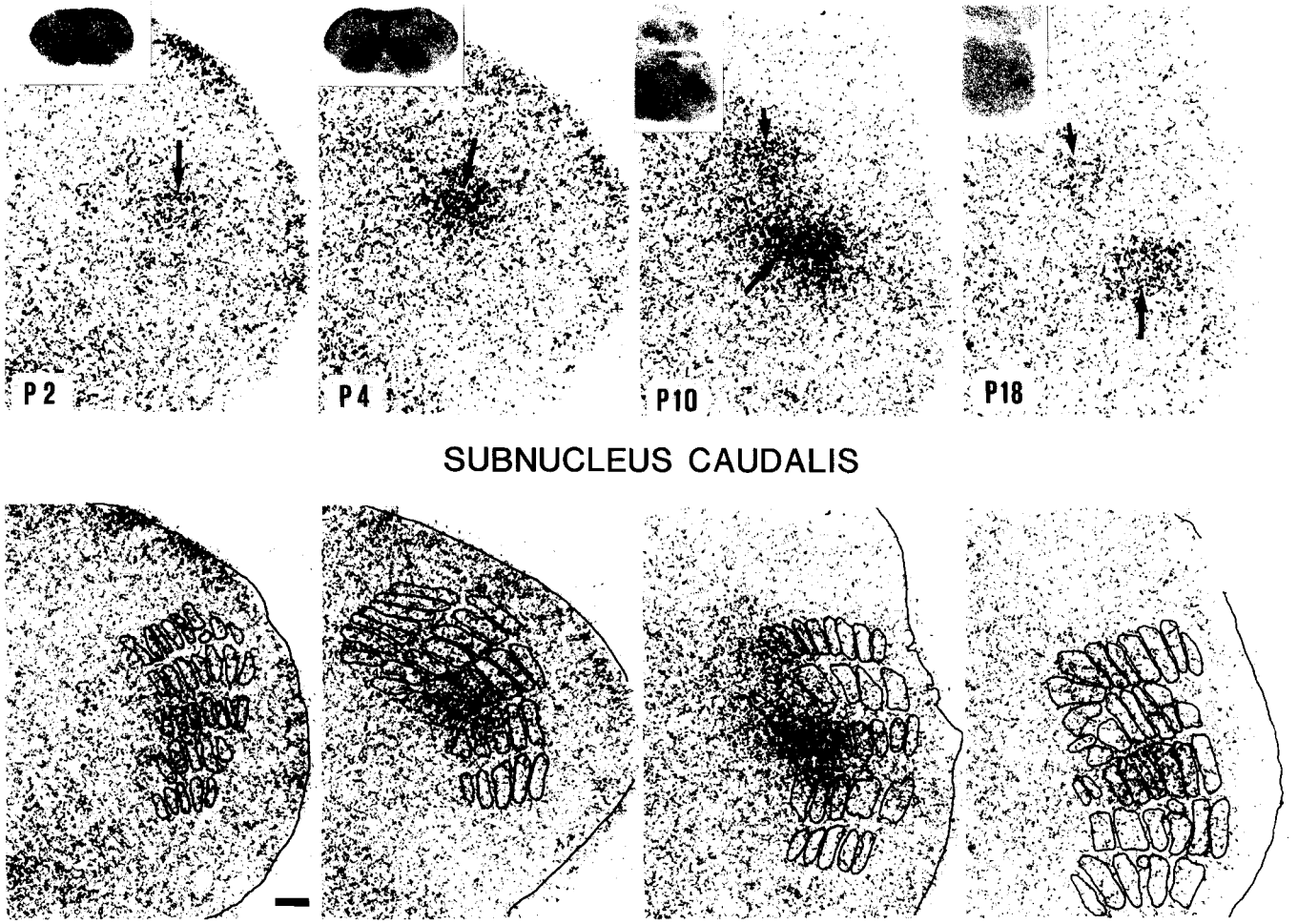

Fig. 2. Left subnucleus caudalis: photomicrographs of autoradiograms of 20 μm thick transverse sections through the brainstems of mice at postnatal days (P) 2, 4, 10, and 18. The photographs in the top and in the bottom row of panels are identical, but in the bottom row, the outlines of CO segments representing the tall, caudal whiskers in rows A to E (from ventral to dorsal) are superimposed on the autoradiograms. These outlines were based on camera-lucida drawings of the CO-segments as seen in the microscope; see Fig. 3 for correspondence between drawings and the photomicrograph of the section stained for CO-reactivity. Follicles of left whiskers C1–3 and E1 were stimulated. The insets in the top row serve to identify the part of the autoradiograms from which the photomicrographs had been taken. At P2 high strength routine stimulation was applied; at P4, P10 and P18, low strength routine stimulation. At all ages shown, there is one area of high DG uptake, located at the medial end of row C (long arrows). At P10 and P18, there is an additional, smaller area, located at the medial end of row E (short arrows). The areas of stimulus-dependent DG uptake extend beyond the CO segments whose whiskers were stimulated. For all illustrations dorsal is up. The bar at lower left is 100 μm and holds for all panels at the larger magnification.

DG uptake was confined to two sites (Fig. 1): a large area covering three segments in row C and a small area covering one segment in row E, both at the lateral ends of the rows. In So (only in two mice) and Np (three mice), one area of stimulus-dependent DG uptake covered a large part of the whisker representation.

At P18, in the three animals studied, the two areas of stimulus-dependent DG uptake, medial in Sc (Fig. 2) and lateral in Si (Fig. 3), were restricted to only a few CO segments in rows C and E. Precisely which whiskers these segments pertained to could not be determined, owing to fragmentation of the individual segments at that age. In the same three mice So did not, but Np did, contain one large area of stimulus-dependent DG uptake (Fig. 6).

In adults, only two animals allowed inspection of the brainstem. In Sc and Si (Fig. 1), using low and high strength stimulation, we again found the large and the small area of increased DG uptake in row C and in row E, respectively. Due to fragmentation of the CO segments, common at this age, it was impossible to attribute areas of stimulus-dependent DG uptake to the individual segments. Both in So and Np, one focus of high DG uptake was located at the lateral boundary of these nuclei.

Two points merit emphasis: (i) in all experiments in which stimulus-dependent DG uptake was observed, the large area at row C and the small area at row E formed continuous rods of variable length. These rods were situated at different positions along the rostro-

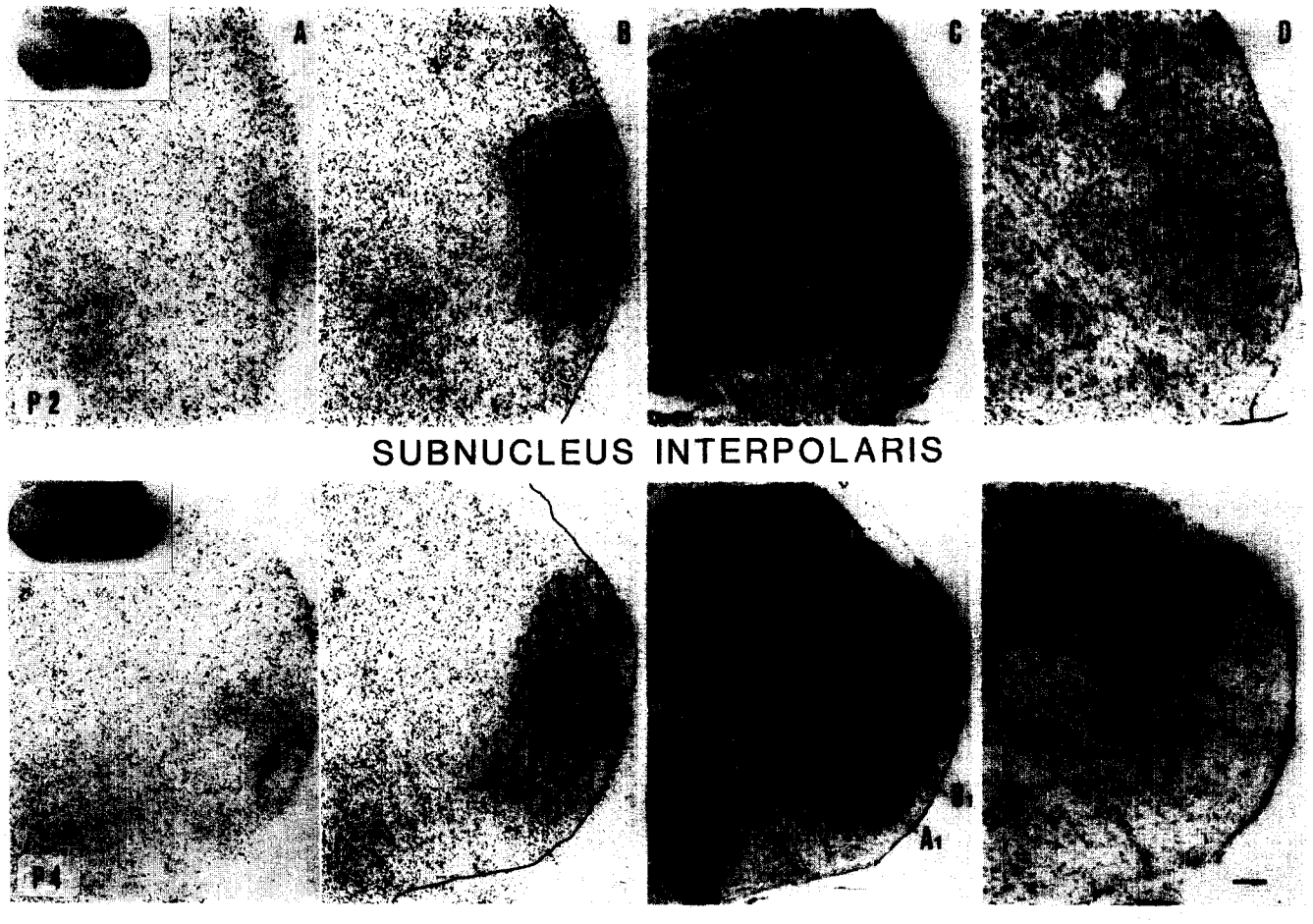

Fig. 3. Left subnucleus interpolaris: photomicrographs of autoradiograms (columns A and B), and of cytochrome oxidase- (CO; column C) and Cresylecht violet- (column D) stained 20 μm thick transverse sections through the brainstems of mice at postnatal days (P) 2, 4, 10, and 18. For each brainstem, the sections shown lie within 80 μm from one another. The photographs in columns A and B are the same, but in column B, the outlines of CO segments representing the tall, caudal whiskers in rows A to E are superimposed on the autoradiograms. The outlines in column B were drawn with a camera-lucida from the sections of which photomicrographs are shown in the corresponding panels of column C. The insets in column A serve to identify the part of the autoradiograms from which the photomicrographs had been taken. The CO segments corresponding to whiskers A1 and B1 are indicated at P4. Follicles of left whiskers C1–3 and E1 were stimulated. At P2 and P4 high strength routine stimulation was applied; at P10 and P18, low strength routine stimulation. At the four ages, there is one area of high DG uptake, located at the lateral end of row C (long arrows in panels of column A), while at P10 and P18, there is an additional, smaller area, located at the lateral end of row E (short arrows). The areas extended beyond the CO segments whose whiskers were stimulated. This mismatch was still present at P10, whereas at P18 the two areas of stimulus-dependent DG uptake are clearly separated. For all illustrations, dorsal is up; the two bars to the right are 100 μm and hold for all panels.

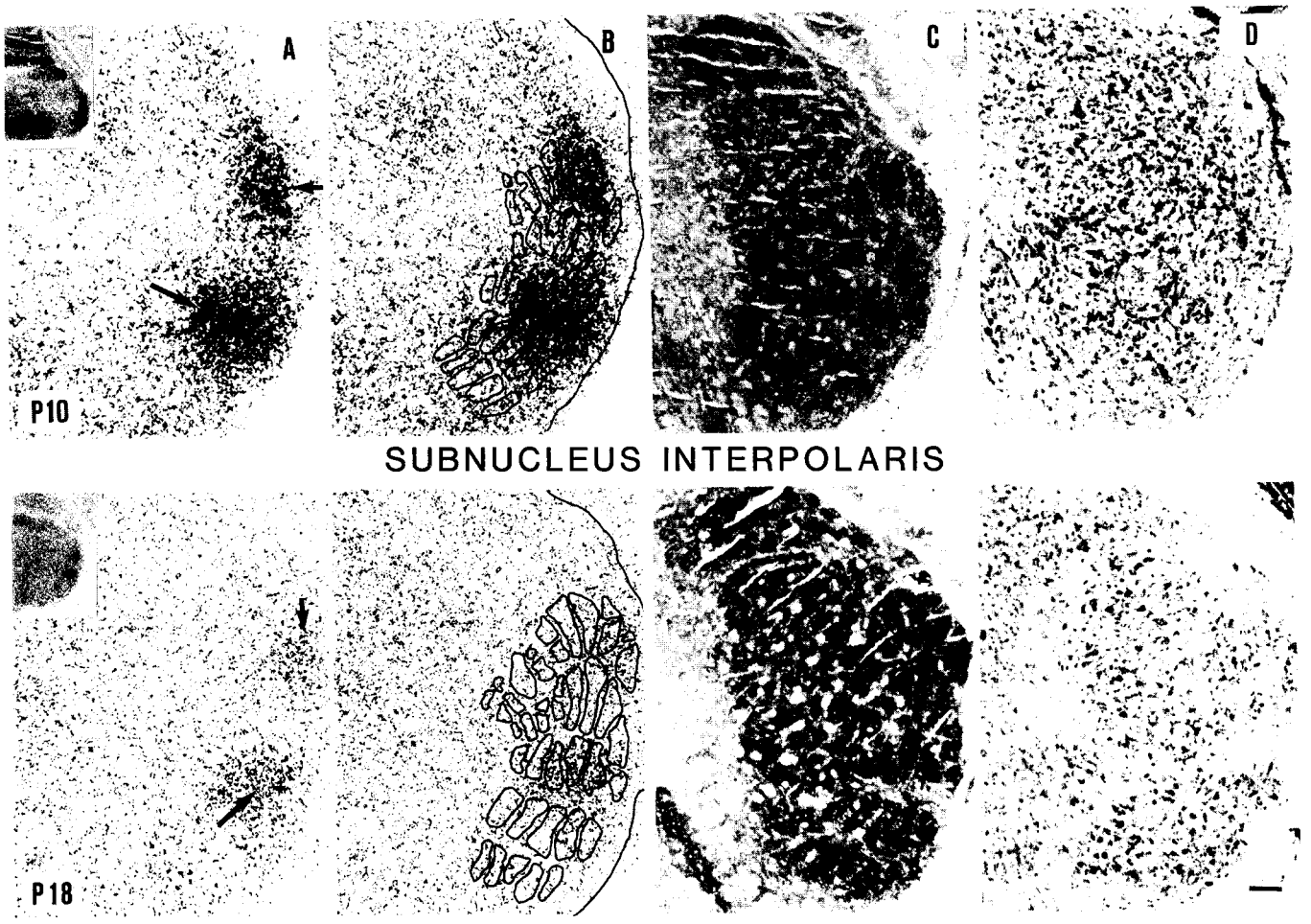

Fig. 3 (continued).

caudal extent of Si and Sc. Both forms of variation occurred at all ages. At the transition from Si to Sc, the rods were never continuous, and their position changed from lateral in Si to medial in Sc. More caudally in Sc, the stimulus-dependent DG uptake was observed to gradually shift in a lateral direction; (ii) from P4 to P10, with low strength routine stimulation, the magnitude of the stimulus-dependent DG uptake in the sensory trigeminal brainstem nuclei increased continuously (for Np, see Fig. 6; for Si, Fig. 1, top row; see also quantitative analysis). It dropped at P13 and later. In Sc and Si of adults, stimulus-dependent DG uptake in the representation of whisker E1 was almost at the level of adjacent non-activated tissue, while in the representations of C1–3 it was weak (for Si, see Fig. 1).

The nucleus ventrobasalis of the thalamus (Figs. 1 and 7)

At P2, we could not find stimulus-dependent DG uptake (Fig. 7), whereas CO segmentation was present.

At P4, a band of stimulus-dependent DG uptake could be observed curving from dorsolateral to ventromedial along the ventral boundary of VB contralateral to stimulation (Fig. 7). The band was found in seven of the ten mice analyzed, which had been exposed to routine and non-routine stimulation.

At P6, stimulus-dependent DG uptake was restricted to the dorsolateral edge of the nucleus. At this age, and at P7, this focus was found in all animals.

At P9, all mice showed one focus of stimulus-dependent DG uptake spanning up to four barreloids per section (Fig. 7). Since the plane of section was coronal, we could not determine which whiskers were represented by these barreloids. We never found a second area of stimulus-dependent DG uptake (which would have corresponded to the representation of E1).

From P10 onward, the magnitude of stimulus-dependent DG uptake dropped considerably (see Quantitative Analysis); at P13, only a small, weak focus was seen (see Fig. 1, center row).

At P18 and in adults, no stimulus-dependent DG uptake could be found, either at low or at high strength routine stimulation. On both sides, overall DG uptake in VB was high.

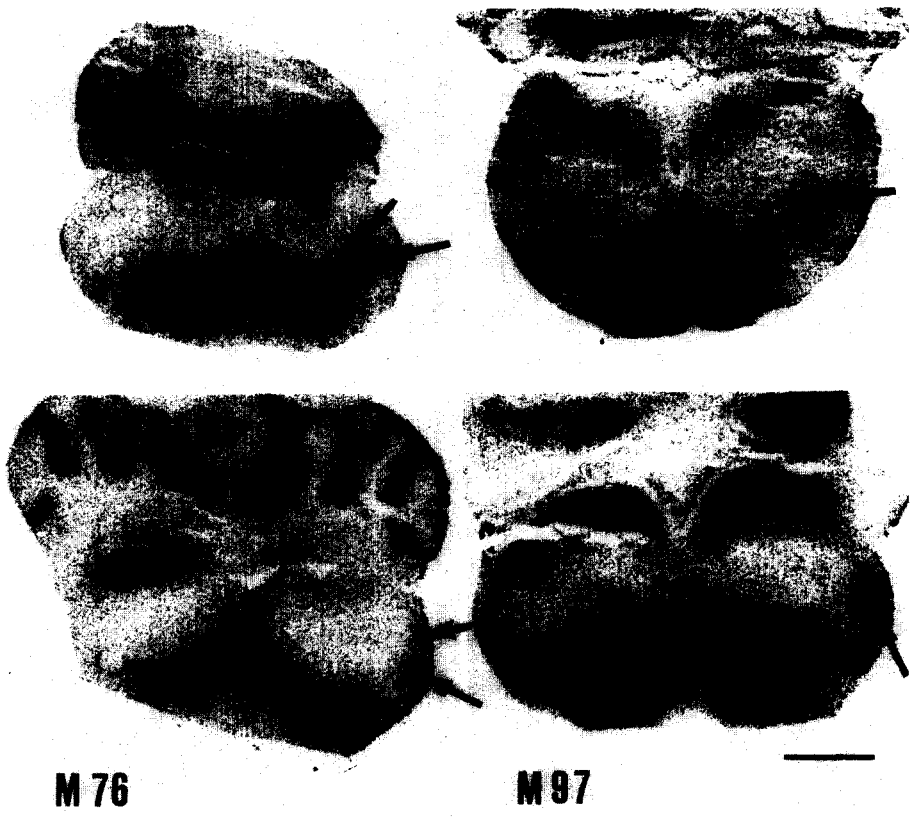

Fig. 4. Results from stimulation with non-routine parameters of mice M76 and M97 at postnatal day 4 (see Table II). DG uptake in subnuclei caudalis (top row) and interpolaris (bottom row) as shown in photomicrographs of autoradiograms of 20 μm thick transverse brainstem sections. Follicles of left whiskers C1–3 and E1 were stimulated. In both animals, DG uptake evoked by the deflection of whiskers C1–3 is clearly visible (long arrows). M76 shows uptake to stimulation of E1 as well (short arrows), which is a unique observation for this age group. Dorsal is up; the left side of the brainstem is to the right. The bar at lower right represents 1 mm and holds for the four illustrations.

Fig. 5. Left subnucleus oralis: photomicrographs of an autoradiogram (A), a cytochrome oxidase-stained section (B) and a Cresylecht violet-stained section (C) of a postnatal day 10 mouse, the same as shown in Figs. 2, 3, and 7. The transverse sections, cut at 20 μm, lie within 80 μm from one another. Follicles of left whiskers C1–3 and E1 were subjected to low strength routine stimulation. The cytochrome oxidase-stained section (B) does not reveal any segmentation. We find one area of stimulus-dependent DG uptake (arrows in A). Orientation: dorsal is up. The bar at lower right of C represents 100 μm and applies to the three panels.

The barrel cortex (Figs. 1, 8 and 9)

At P2, we did not detect stimulus-dependent DG uptake.

At P4, where CO segmentation first appeared, we found high DG uptake in a thin subpial zone in the parietal cortex. It appeared of equal magnitude on both sides (Fig. 1, column 'P4'). It was not confined to the incipient BC but extended occipitally, and therefore, we do not relate this DG uptake to stimulation. The same observation was made at P5 and P6.

At P7, in three of six mice that had been stimulated with low strength routine stimulation, and whose brains were cut coronally, we found the earliest stimulus-dependent DG uptake in BC. The autoradiograms showed

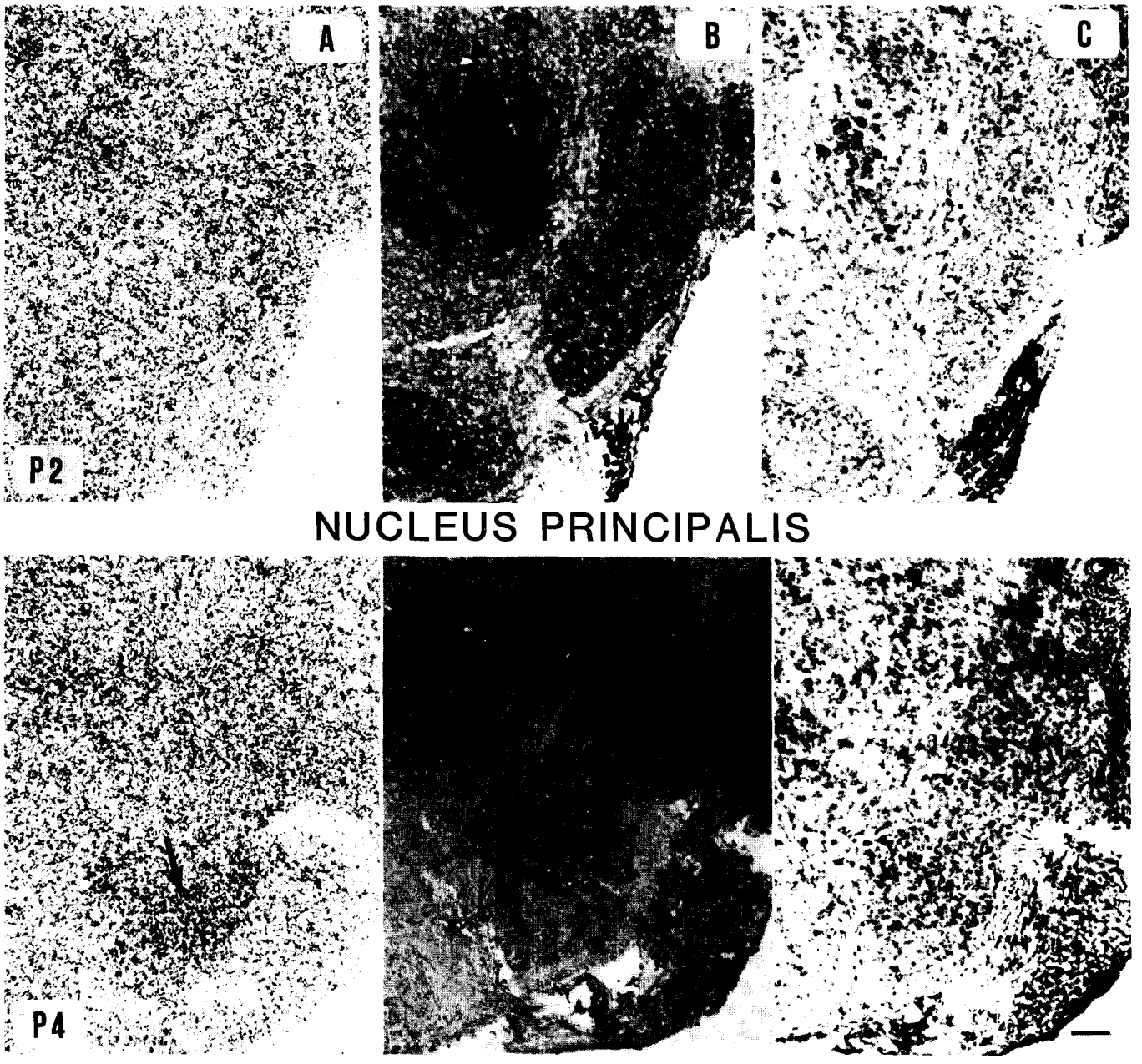

Fig. 6. Left nucleus principalis: photomicrographs of autoradiograms (column A), and of cytochrome oxidase- (CO; column B) and Cresylecht violet- (column C) stained 20 μm thick transverse sections through the brainstems of mice at postnatal days (P) 2, 4, 10, and 18. In each row, the sections – of which the same region are depicted – lie within 80 μm from one another. Follicles of left whiskers C1–3 and E1 were stimulated. At P2 and P4, high strength routine stimulation was applied; at P10 and P18, low strength routine stimulation. At P2, there is no stimulus-dependent DG uptake. At P4 and P10, there is *one* diffuse area of DG uptake ventral in the nucleus (arrows in column A). At P4, it covers the 5 rows of CO segments representing whisker rows A to E (as indicated in photomicrographs of the P10-animal in column B). We cannot determine whether this DG uptake is due to stimulation of whiskers C1–3 only, or to that of E1 as well. At P10, an area of marked DG uptake is located at the ventromedial border of the nucleus. The magnitude of the stimulus-dependent DG uptake is higher in P10 than in P4; at P18, the uptake has nearly vanished (arrows in column A). All illustrations are oriented so that dorsal is up, and shown at the same magnification; bars at the right represent 100 μm.

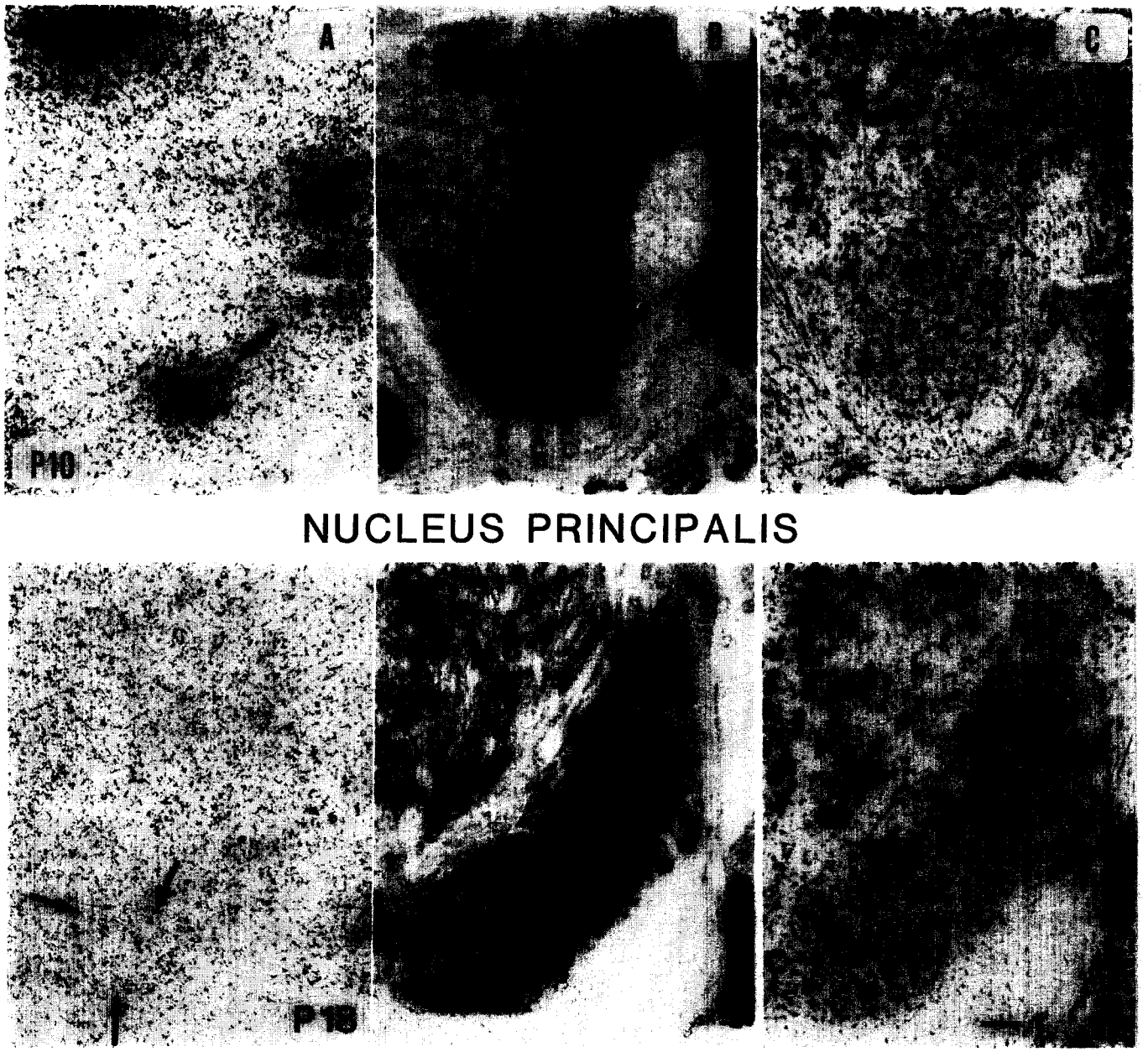

Fig. 6 (continued).

a small, well-defined region of increased DG uptake in BC, contralateral to stimulation (Fig. 1, bottom row). It comprised layer IV and lower layer III (Fig. 8). Of the three mice whose hemispheres were cut tangentially, only one, stimulated with high strength routine stimulation, showed an area of stimulus-dependent DG uptake. This area comprised barrels α, β, γ, δ, A1, A2, B1–3, C1–4, D1–5 and E1–4 (Fig. 9).

At P9, in all three experiments the hemispheres were cut coronally. In BC contralateral to stimulation, layer IV contained the highest stimulus-dependent DG uptake. The coronal sections did not allow us to determine whether the uptake was restricted to barrels C1–3 and E1. In deep layer V, there was another focus of stimulus-dependent DG uptake, lower in magnitude than that in layer IV. Still less elevated stimulus-dependent DG uptake stretched radially between these two foci and extended into layers II and VI, thus forming a radial 'metabolic column' flanked medially and laterally by bands of DG uptake lower than that in BC beyond these bands.

At P10, the four animals studied showed stimulus-dependent DG uptake in BC. On autoradiograms from tangential sections, two areas of stimulus-dependent DG uptake were limited to contralateral barrels C1–3 and E1 (Fig. 9). The two areas covered the barrels in question together with the adjacent septa. DG uptake in barrels C1–3 was higher than that in barrel E1 (see

Quantitative Analysis). Activated barrels C1–3 were surrounded by a band of depressed DG uptake about one barrel wide; barrel E1 appeared to be surrounded by a similar, though less pronounced, band. DG uptake in the barrels of row D was lower than that in the barrels of row B (Fig. 9, P10). The zones of diminished DG uptake extended into the supragranular layers. Autoradiograms from coronally sectioned hemispheres displayed a radial metabolic column, including foci of high DG uptake in layer IV and deep layer V (Fig. 1), not unlike the situation at P9. However, two distinct DG columns that may represent whiskers C1–3 and E1 separately were not observed.

At P13 the magnitude of stimulus-dependent DG uptake in layer IV decreased (see Quantitative Analysis). In autoradiograms from coronal sections, the metabolic column became more accentuated, due to an increase in DG uptake in supra-and infragranular layers (Fig. 1, P13, bottom panel).

In adults, in the coronal plane, the columnar pattern of stimulus-dependent DG uptake remained, although the focus in layer V had become less pronounced. In the tangential plane, stimulus-dependent DG uptake remained restricted to the barrels whose whiskers were stimulated. The surrounding band of depressed DG uptake, while present, was never as clear as at P10.

Fig. 10 summarizes when during postnatal development the first signs of stimulus-dependent DG uptake in each station were observed and how they are related to the appearance of the whisker representations as observed in CO- and Nissl-stained sections. In each station the onset of stimulus-dependent DG uptake lagged behind the first appearance of the morphological whisker maps. The delay was 2 to 3 days shorter for

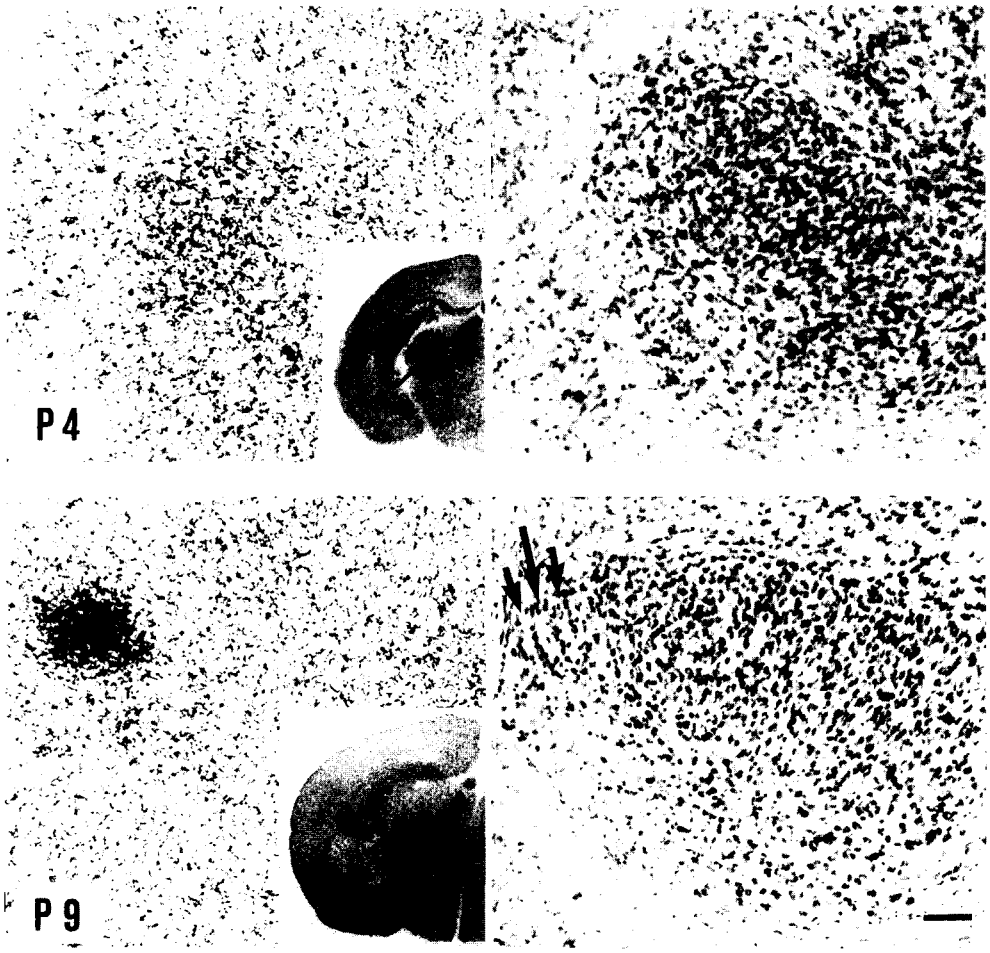

Fig. 7. Nucleus ventrobasalis of the right thalamus: photomicrographs of autoradiograms (left column), and of Cresylecht violet-stained 20 μm thick coronal sections (right column) through the brains of mice at postnatal days (P) 4 and 9. In each row of panels, the sections lie within 80 μm from one another. In the left column, the low magnification insets show those parts of the autoradiograms from which the photomicrographs were taken (arrows point at areas of stimulus-dependent DG uptake). Follicles of left whiskers C1–3 and E1 were stimulated. At P4, high strength routine stimulation was applied; at P9, low strength routine stimulation. At P4, the autoradiogram shows one diffuse area of stimulus-dependent DG uptake. At P9, the crisp, dark area covers only 3 to 4 barreloids a few of which can been seen at arrows in the right column. Illustrations are oriented so that dorsal is up and lateral to the left. Bar – bottom right – holds for all panels and represents 100 μm.

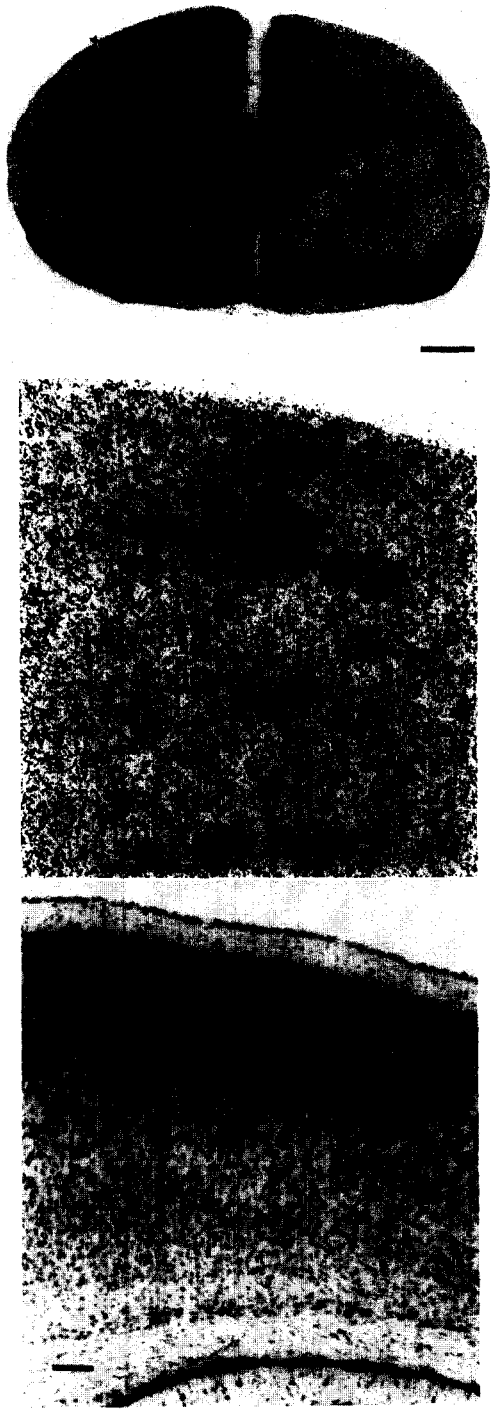

Fig. 8. Barrel cortex at postnatal day 7; top: autoradiogram (same as in Fig. 1 at 'P7', bottom row), taken from a 20 μm thick coronal section of the parietal cortex; center: detail of autoradiogram shown above; bottom: photomicrograph of the corresponding detail from the Cresylecht violet-stained section. The arrowheads in the top panel correspond to the arrows and arrowheads in the center and the bottom panel and delineate the area of stimulus-dependent DG uptake. Follicles of left whiskers C1–3 and E1 were stimulated according to the low strength routine paradigm. Comparison of the autoradiogram and the Nissl-stained section shows that increased DG uptake covers two adjacent barrels (the arrows in lower panel point to the walls surrounding them). Radially, stimulus-dependent DG uptake spans layer IV plus part of layer III. Bars: 1 mm (in top panel), and 200 μm (in bottom panel; this bar holds for center and bottom panel). Note that photomicrographs in center and bottom panel are slightly rotated clockwise with respect to top panel.

DG uptake evoked by the stimulation of whiskers C1–3 than that evoked by the stimulation of whisker E1. For the possible effect of modification of the stimulus parameters upon the appearance of stimulus-dependent DG uptake, see Discussion.

Quantitative analysis

Transmittance of light, measured at activated and at the neighboring non-activated sites, ranged from 0.36 to 0.93. Mean optical densities (mODs) lay between 0.07 and 1.02, and radioactivity content in brain tissue between 49 and 716 nCi/g. In this range, mOD was linearly correlated with radioactivity content ($r = 0.964$, $P \leq 0.0001$). Therefore, in our case, the measurements used to calculate R lay in a range in which OD was directly proportional to radioactivity in brain tissue, which in turn is directly proportional to DG uptake.

In Fig. 11, for each age, either the median R of one animal, or, where several mice could be analyzed, the median of median Rs of the mice in that age group, were plotted. The stations analyzed were Si, VB and BC. The values obtained for the areas corresponding to stimulated whiskers C1–3 and E1 were kept separate.

Subnucleus interpolaris. DG uptake evoked by stimulation of whiskers C1–3 peaked at P7. Activation to stimulation of whisker E1 was highest at P7 and P10. None of the differences between ages reached significance in the Wilcoxon/Kruskal–Wallis test. The response to stimulation of whiskers C1–3 is on average 20% higher than that to stimulation of whisker E1.

Nucleus ventrobasalis of the thalamus. Here, stimulus-dependent DG uptake at P7, P9 and P10 was significantly higher than that at P4, P11 and P13. In this nucleus, DG uptake evoked by stimulation of whiskers C1–3 and E1 could not be measured separately.

The barrel cortex. DG uptake in barrels C1–3 was highest at P10 and lowest at P7 and P18; only differences between P10 and P7, and between P10 and P18 were significant. DG uptake in barrel E1 could be measured at P10 and in adults. In both groups, activation in barrels C1–3 was higher than that in barrel E1.

Comparison between stations. In mice between P7 and P18, DG uptake evoked by stimulation of whiskers C1–3 was always higher in Si than that in BC. The highest stimulus-dependent DG uptake in Si (at P7), was 1.3 times higher than that in VB (at P10) and in BC (at P10). In adults, this relationship reversed and activation in BC surpassed that in Si. In VB, activation

at P7 and P9 was higher than that in BC; this inversed as of P10.

In summary, during postnatal development stimulus-dependent DG uptake reaches peaks in Si, VB and BC. In the three stations, the peaks were followed by a decline, which was most outspoken in Si. In Si and BC, the magnitude of DG uptake evoked by stimulation of whiskers C1–3 was always higher than that evoked by stimulation of whisker E1. This difference could not be tested for statistical significance (see Materials and Methods).

DISCUSSION

Four major observations of this study will be discussed:

(I) The onset of stimulus-dependent DG uptake in the whisker-to-barrel pathway follows a time sequence from brainstem to cortex.

(II) At the earliest signs of stimulus-dependent DG uptake, the pattern of uptake reveals a rough somatotopic representation of the whisker follicles in brainstem and cortex.

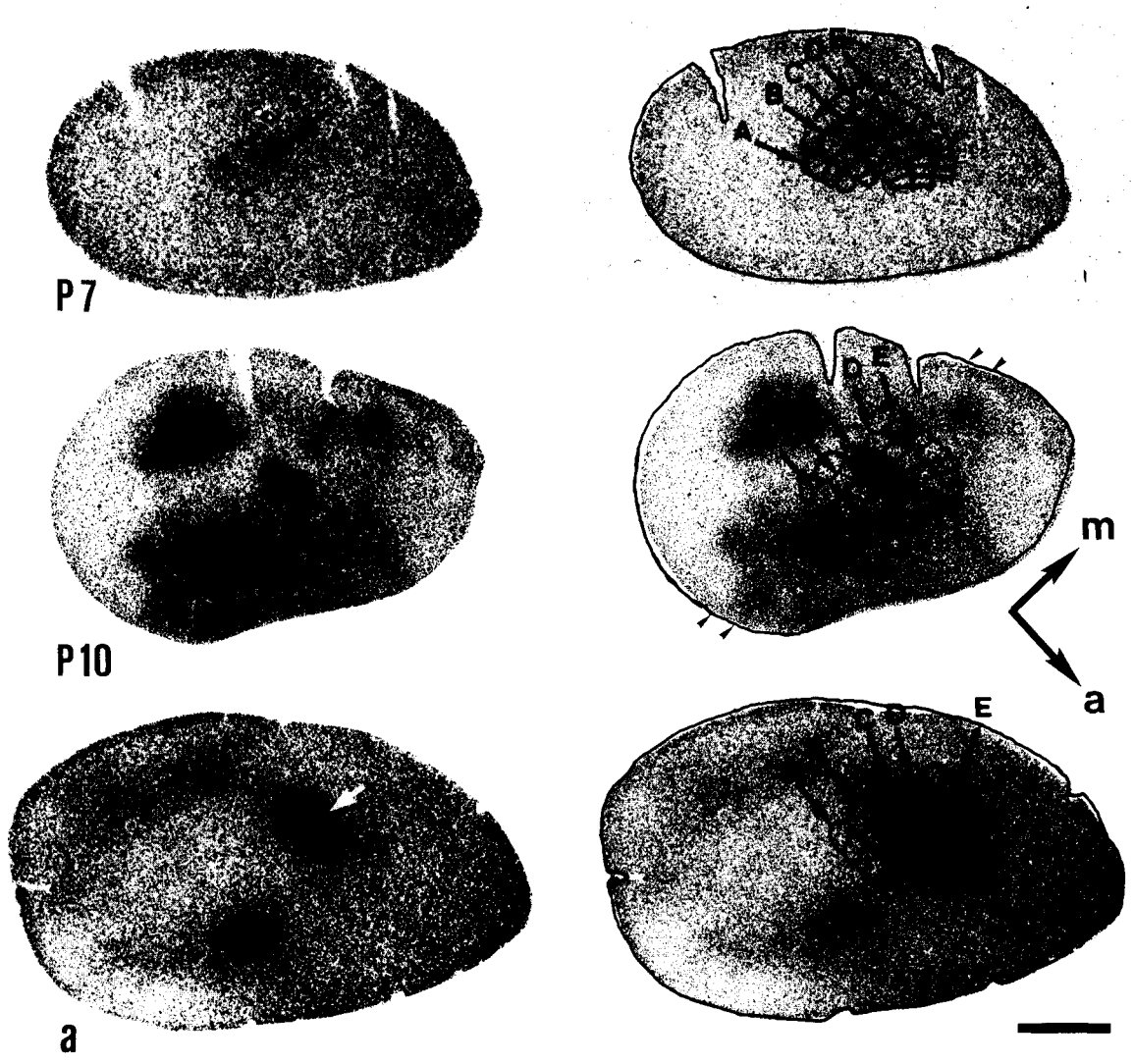

Fig. 9. Right barrel cortex: autoradiograms of 20 μm thick tangential sections from the parietal cortex of mice at postnatal days (P) 7, 10 and 60 (adult, a). In each row of panels a pair of identical autoradiograms is shown, but on those in the right column camera lucida-drawings of the barrels, reconstructed from the corresponding series of Cresylecht violet-stained sections, are superimposed. The caudalmost barrel of each row is labeled A to E from lateral to medial; caudal to, and between, the rows are the barrels of the straddlers α–δ. Each autoradiogram was taken from the middle section of the series from which the barrelfield was reconstructed. Follicles of left whiskers C1–3 and E1 were stimulated. At P7 as well as in the adult, high strength routine stimulation was applied; at P10, low strength routine stimulation. At P7, stimulus-dependent DG uptake is diffuse (arrow in left panel); in this section it spans barrels α, β, γ, A1, A2, B1–3, C1–4, and D1. Adjacent sections (not shown), have high DG uptake in barrels γ, D2–5 and E1–4. At P10, high DG uptake is limited to barrels C1–3 (arrow in left panel), and less increased DG uptake to barrel E1 (arrowhead in left panel); note the barrel-wide rim of depressed tracer uptake surrounding barrels C1–3. In the adult, the high DG uptake remains restricted to barrels C1–3 (white arrow in left panel) and E1 (not on the autoradiogram shown), i.e. the barrels whose whiskers were stimulated; the magnitude of the DG uptake in barrel E1 is less than that in barrels C1–3. Compass: a, anterior; m, medial. Bar represents 1 mm. Compass and bar hold for the six panels.

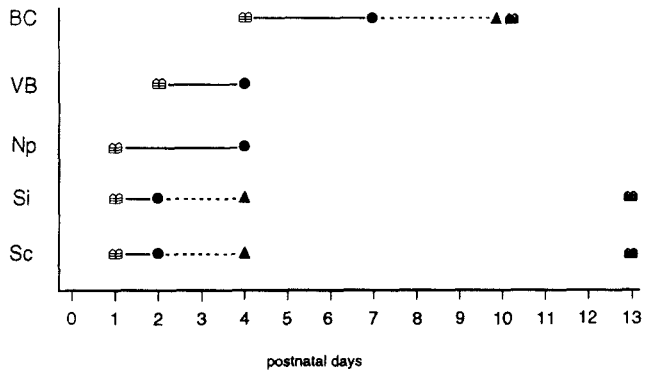

Fig. 10. Diagram summarizing some salient events in the postnatal development of five stations in the whisker-to-barrel pathway (Sc, subnucleus caudalis; Si, subnucleus interpolaris; Np, nucleus principalis; VB, nucleus ventrobasalis; BC, barrel cortex). Time in postnatal days (P; P0 = day of birth) is plotted on the abscissa. Empty segmented icons indicate the first appearance of CO segments representing the whisker map in a given station; those pertaining to the brainstem nuclei are derived from the work of Ma[40]. Dots indicate the first appearance of stimulus-dependent DG uptake, which may stem from both stimulation of whiskers C1–3 and stimulation of whisker E1 and from high or low strength routine stimulation. Triangles indicate the appearance of a small area of high DG uptake related to the stimulation of whisker E1, separate from the large area of high DG uptake related to the stimulation of whiskers C1–3. The triangles at P4 reflect data obtained from other than routine-stimulation (Table II). Stippled segmented icons indicate the first day on which areas of stimulus-evoked DG uptake and the representations of the stimulated whiskers could, in the present study, be shown to match. The horizontal line segments emphasize that CO segmentation develops before the onset of stimulus-dependent DG uptake; the dashed line segments, that barrel E1, as a distinct entity, responds later than barrels C1–3.

(III) Early in postnatal development, the areas of stimulus-dependent DG uptake in subnuclei caudalis and interpolaris as well as in barrel cortex were larger than the corresponding morphological whisker representations, whereas later a good match was established.

(IV) In all stations a maximum of stimulus-dependent DG uptake was observed at about P10, followed by a decrease.

I. The time sequence of the onset of stimulus-dependent DG uptake in the whisker-to-barrel pathway

The occurrence of stimulus-dependent DG uptake in the stations along the pathway within an individual varied considerably between animals. Possible factors here are: while all mice used are from ICR-origin, they did not form a genetically homogeneous group; moreover, as mentioned in Material and Methods, animals used may have been 24 h older than the age assigned to them; a third factor resides in the stimulus applied, where head movement could have induced variability between mice. However, notwithstanding this interindividual variability, one tendency is clear: in development the onset of DG uptake evoked by whisker stimu-

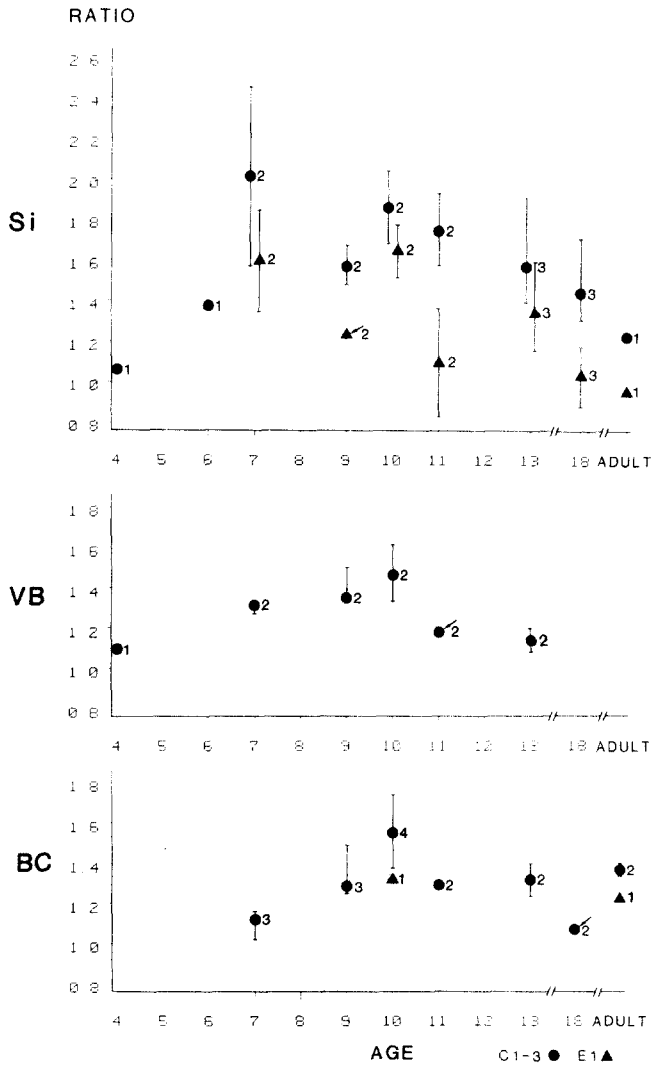

Fig. 11. Graphs showing the age dependence of the relative magnitude of stimulus-evoked DG uptake in subnucleus interpolaris (Si), nucleus ventrobasalis of the thalamus (VB) and barrel cortex (BC). Only results of experiments using low strength routine stimulation are plotted. The magnitude (ordinate) is expressed as the ratio between the mean optical density taken from the area of stimulus-evoked DG uptake and the mean optical density taken from an immediately neighboring area within the same station. In BC, measurements were taken from layer IV. In the mice whose hemispheres were sectioned coronally, the site of barrels C1–3 and barrel E1 could not be identified with certainty. Here, the large area of increased DG uptake was taken to represent the activation in barrels C1–3. At P10 and in adults some hemispheres were cut tangentially. In these experiments, metabolic responses to stimulation of whiskers C1–3 and E1 could be distinguished and separate readings were taken. DG uptake related to the stimulation of whiskers C1–3 (dots) and to stimulation of whisker E1 (triangles) are plotted separately. This convention was also used in the display of data related to Si. For VB the data were considered to represent stimulus-dependent DG uptake in barreloids of row C. The age (abscissa) is expressed in postnatal days (P) (adult is P45 and P69). Note that stimulus-dependent DG uptake drops in all stations after P10. Data points pertain to the median ratio of each age group; bars indicate ranges. Arrows indicate data points with ranges smaller than the symbol. Numbers within the graphs indicate the number of mice analyzed in any one group. At ages represented by one mouse, the data point without range bar is the median result of that individual. At ages at which the ranges for C1–3 and E1 overlap, data points are spaced horizontally.

lation follows a sequence from brainstem, via thalamus, to cortex. Once established in a station, the metabolic response remains present, except in thalamus where it may be present but masked by the high uptake in all of VB. Although the onset of stimulus-dependent DG uptake in a station may advance by a few days with changing stimulus parameters, the *sequence* of onset along the pathway could not be modified by changing them. Interestingly, in our study there was no variability in the presence of CO-segmentation between the animals of any given age.

Does absence of a stimulus-dependent DG uptake to whisker deflection during development signify the absence of functional activity due to immaturity of that part of the pathway? Or does it signify the use of a substrate of neuronal energy metabolism other than glucose? With respect to the latter possibility, ketone bodies may well be one such alternative source of energy[16]: in the early postnatal rat it has been shown that their contribution to the total brain energy metabolism can be as high as 30%[13]. Thus, in our experiments the preferential use of ketone bodies might have prevented DG uptake evoked by the stimulation of whiskers in thalamus (at P2) and cortex (at P2–P6). This attractive notion does not receive support from a pilot study in which we found that the stimulation of whiskers of P4 mice injected with a radioactively labeled ketone body, [1-^{14}C]D-β-hydroxybutyrate, did not demonstrate a stimulus-dependent uptake in VB and BC. However, there was such uptake in Sc and Si[48]; regions that also showed stimulus-dependent DG uptake as demonstrated in the present study.

In adults, the magnitude of DG uptake in barrel E1 was shown to be independent from the number of simultaneously stimulated whiskers in row C[43]. In the design and the discussion of the present study we have assumed that during maturation DG uptake evoked by the stimulation of whisker E1 was independent from that evoked by the stimulation of whiskers C1–3 (and vice versa).

The earliest stimulus-dependent DG uptake in the stations of the whisker-to-barrel pathway was obtained by stimulating whiskers C1–3. In all stations DG uptake to stimulation of whisker E1 lagged behind by two to three days. Where there was DG uptake in the representation of E1, it was lower than that in the representation of C1–3. The difference is preserved to adulthood, where it persists even under increasing stimulus strength[46]. The time lag and the difference in magnitude of DG uptake indicate that in infant mice, as in adults, there is a mutually reinforcing effect on metabolic responses by the deflection of adjacent whiskers in one row. This observation may well be explained by the model proposed by McCasland et al.[42]. It would be interesting to study whether stimulation of a number of adjacent whiskers across rows leads to a similar effect.

Using routine stimulation, stimulus-dependent DG uptake in the representation of E1 appears at P7. However, by reducing the burst rate to a third of routine and doubling the total duration of the stimulation period from 45 to 90 min (see Table II), we obtained DG uptake in Sc and Si at P4 upon stimulation of a *single* whisker follicle (M76 in Fig. 3), but could not influence cortical metabolism *. With single- and multi-unit recordings in SI of anesthetized rats, a higher degree of habituation of cortical units upon peripheral stimulation was shown at P5 and P6 than in adults[1]. The lower stimulus rate and/or longer interburst pauses in experiment M76 may have prevented such habituation in the immature pathway, here studied while the animal was unanesthetized. This mode of stimulation may have permitted to drive brainstem nuclei more effectively, which may explain the appearance of the functional representation of whisker E1 in M76. This observation might suggest that, indeed, for all ages investigated alternative stimulation paradigms could have been applied – obviously an impossible undertaking. In comparison with the low strength routine stimulation, the high strength stimulation gave more consistent results at P4, probably because the latter stimulus drove cells more effectively and/or increased the number of driven cells.

When confronted with the results of other studies, there is a problem in counting postnatal days and in the determination of the moment of birth. The discrepancy of one day between laboratories which define the birthday of a litter as postnatal day 1[1,20,40,67,68], and laboratories, including our own, which define the birthday as postnatal day 0[4,5,34,36,80], can be accounted for. As to the second point, only few authors define the precision with which the moment of detection of a litter was determined, and whether postnatal days were counted in calendar days or, as done in this study, in sets of 24 h, each set beginning at the moment of detection. Together, this may cause a discrepancy of up

* Our finding that stimulus-dependent DG uptake is present 90 min after injection is in harmony with the finding that adult guinea pigs, exposed to pure tones, show tone-specific DG uptake in the inferior colliculus 90 min after injection[72]. Both findings support the reports on a slow hydrolysis of DG-6-phosphate by phosphatase[50,61,62] and contrast with those claiming rapid hydrolysis of DG-6-phosphate[18,22,25,55].

to two days for a given postnatal day. Throughout this report we tried to match the observations by other laboratories to our age scheme. Another factor contributing to the uncertainty incurred when trying to match dates, is that some observations on the maturation of the pathway in question derive from rats, and others from mice. All these factors may have contributed to the reported variations in the onset of events during postnatal development.

In our CO-stained preparations, segmentation was already present in Sc, Si, Np and VB at P2, while in BC it was first seen at P4. Ma[40] observed segmentation in Sc, Si and Np to arise in CO-stained preparations of mice brainstem first at P1. These observations are in harmony with the finding that, in rat, segments of high succinyl dehydrogenase (SDH) activity in Np develop between birth and P3[21]. In VB of mice, the first signs of segmentation as seen in CO-stained preparations are observed at P2[80], whereas in SDH-stained preparations of rat and mouse, segmentation was first reported at P4[5]. We cannot explain this discrepancy (but see previous paragraph). In BC, SDH-stained sections from rats show that segmentation develops between P3 and 6[34]. This is in accord with the first appearance of barrel hollows in mice between late P3 and P4, observed in Nissl-stained sections[53] and with the presence of densely CO-stained hollows at P4 in our preparations. Comparing the onset of stimulus-dependent DG uptake with the appearance of visible segmentation in the stations of the whisker-to-barrel pathway, we note that the functional maturation in Np, VB and BC lagged behind the establishment of CO segmentation by several days. In Sc and Si, such a comparison could not be made for, as mentioned earlier, we did not analyze animals younger than P2. This time lag between segmentation and onset of function may indicate that the appearance of functional synapses follows pattern formation in the whisker-to-barrel pathway.

We have applied CO- and Niss-staining to visualize the central whisker representations, since both techniques could be combined with the autoradiographic DG method in the same animal. In cortex and in thalamus the results obtained with the CO- and Nissl staining agree; in brainstem we relied on CO-material only: in Nissl-material we could not discern whisker representations in consecutive sections. An occasional clustering of cell bodies, more or less in register with the CO-patches, was observed, but virtually never found back in adjacent section. We were not able to confirm the observations by Ma and Woolsey[41] and by Ma[39,40] who obtained, in transverse Nissl-stained brainstem sections, structures Ma[39] termed barrelettes, and interpreted as whisker representations. The difference between those observations and ours may be explained by differences in section thickness and histological procedure; and by differences between the strains of mice used. Other methods have allowed the visualization of the whisker representation in the barrel cortex at earlier stages of postnatal development than described here[7,11,29,31,51,70,81]. These earlier patterns increase the time lapse between the appearance of morphological signs of segmentation and the onset of stimulus-dependent DG uptake.

The time lag between the onset of DG uptake evoked by the stimulation of three whiskers and the onset of that evoked by the stimulation of a single whisker in brainstem and cortex points to the possibility that the onset of stimulus-dependent DG uptake observed in the present study may be specific for the type of stimulation applied. A case in point is given by our analysis on P4: while routine stimulation did not result in activation of the E1 representation in the sensory trigeminal brainstem nuclei, non-conventional stimulation did (Table I). Alternatively, we cannot rule out that the mechanical stimulation of *all* whiskers would have resulted in neural responsivity in thalamus and cortex at ages earlier than we observed, perhaps even at a time that the morphological whisker maps are not yet laid down. Therefore, the possibility that neural activity emanating from the stimulation of all whiskers plays a role in the development of morphological whisker representations is an interesting point. Studies that address this issue have shown that blocking neuronal activity postnatally does not prevent the formation of the whisker pattern in the central stations of the trigeminal pathway[8,23].

Another question concerns the role of experience-dependent neural activity in neonatal plasticity. Up to P6, permanent damage to whisker follicles in mice[20,28,66,78] and rats[34] causes morphological changes in the barrel cortex: the lesion of follicles in row C led to an enlargement of the adjacent rows (i.e. rows B and D) and to the absence of barrels of row C. In the present study, the first stimulus-dependent neural activity in BC occurred after the critical period for these structural modifications was over. It has been proposed that stimulus-dependent DG uptake in a particular station is related to spiking activity in the presynaptic element in that station[32,33,57]. Opting for this hypothesis, the absence of stimulus-dependent DG uptake in one station, together with the presence of such response in the preceding station may be due to a subthreshold number of spikes traveling from the lower station to the next one up. Interestingly, the onset of stimulus-dependent DG uptake may occur long after the arrival of thalamocortical axons in the immature

cortex[31,58] and after the end of the 'critical period' of that station.

P7 was the earliest age at which stimulus-dependent DG uptake was seen in BC. In coronal sections, the highest DG uptake was in layer IV, inside the barrels. Layer III showed DG uptake, too, in register with that in the barrels, but of smaller magnitude. This pattern of stimulus-dependent DG uptake is similar to that found in rats at P6[36]. Our study agrees with these findings, in that subsequently a second focus of stimulus-dependent DG uptake appears deep in layer V. While in the rat this occurs at P8, we detected the second focus at P9. Finally, both in rats and mice, a further expansion of stimulus-dependent DG uptake into supra- and infragranular layers was seen to occur later in development, forming a 'metabolic column'. In the rat the onset of stimulus-dependent DG uptake in the cortical plate was as early as about P4, i.e. 3 days earlier than in mice. Rats appear to run ahead of mice in another aspect of cortical maturation: the onset of evoked potentials in the somatosensory cortex elicited by electrical stimulation of the trigeminal nerve or of the thalamus is at P3 in rats[67] and at P7 in mice[68].

The appearance of high stimulus-dependent DG uptake in deep layer V at P9 in mice agrees with the finding in adults that, whereas the majority of the thalamic afferents terminate in lower layer III and layer IV, they do have branches terminating in deep layer V and upper layer VI[6,30,74]. Therefore, these two foci of stimulus-dependent DG uptake may reflect spiking activity in the terminals of thalamocortical projections. The endings of these deeper collaterals may have grown out, or may have become functional, two days later than the prime terminals in layers III and IV. The appearance of a column of stimulus-dependent activity reaching from layer II to layer VI, first seen at P10, could be due to a further spread of thalamocortical terminals into layers II, superficial V, and VI. But only very few of these endings have been found in adults[74]. Thus, activity of thalamocortical terminals alone is not likely to be the basis for the continuous 'metabolic column' in adults. The establishment of such a column would rather point to the functional maturation of intracortical connections, thus implying activation of cortical interneurons. Indeed, such interneurons have been postulated to play a role in limiting the size of receptive fields of neurons in layer IV of the barrel cortex of rats[60].

II. The somatotopic organization of the stations of the pathway

As pointed out in the Introduction, an important property of all but one of the stations of the whisker-to-barrel pathway is that representations of individual whisker follicles are visible in histological sections. We observed stimulus-dependent DG uptake in each station, and for Sc, Si and BC we confirmed that somatotopically organized functional maps exist. In brainstem relays, CO segments representing single whisker follicles were observed in mice of up to P13. From P18 onwards we were unable to delineate the representations of individual whisker follicles owing to the fragmentation of CO segments. However, the identification of rows remained possible.

Belford and Killackey[5] were the first to propose an orderly representation of whisker follicles in Sc and Si of rats and mice. They based themselves on the pattern of SDH segments. The arrangement of the large segments in 5 rows and an irregular cluster of small segments located dorsomedially to these rows, led the authors to the conclusion that the 5 rows of large segments represent, from ventral to dorsal, rows A to E of the large caudal whiskers, while the clustered small segments represent the follicles of the small sinus hairs near and in the mouth. In his study in rats, using transganglionic transport of HRP administered to the proximal stumps of transected follicular nerves, Arvidsson[2], observed that the orientation of the follicle representation within rows is reversed in Sc with respect to that in Si. Recordings from individual afferents in the descending tract of the trigeminal nerve to Sc[27] and Si[26] of the adult rat, followed by the tracing of the morphologically identified fibers and their terminals, demonstrated that in each subnucleus the follicles are represented in cylinders of afferent terminals resembling the cylinders of SDH and CO activity. In agreement with Arvidsson's description, the cylinders of terminals representing the caudalmost whiskers in each row were located at the lateral boundary of Si and at the medial boundary in the rostral part of Sc; moving caudad in Sc, the representations of caudal whiskers progressively shifted laterally.

In Si and Sc, the large area of high DG uptake corresponding to the representation of whiskers C1–3 (where present), covered part of the center row of large CO segments; the small area (where present), corresponding to whisker E1, covered part of the dorsalmost row. These findings confirm the ventral-to-dorsal representation of rows A to E in both subnuclei. The regions of stimulus-dependent DG uptake commonly do not cover the entire rostro-caudal extent of Si and Sc, which may be due to the influence of other inputs to the subnuclei in question. We are currently investigating this interesting notion by studying the role of the projection from BC on patterns of stimulus-dependent DG uptake in Sc and Si[12].

In Si, the areas of stimulus-dependent DG uptake were located at the lateral boundary of the subnucleus; rostral in Sc, at the medial boundary. More caudal in Sc, we noticed a medial-to-lateral shift of the foci of high DG uptake progressing from rostral to caudal. These observations are in harmony with the description of the organization of the whisker representation in Si and Sc[2,26,27].

In So, only one area of stimulus-dependent DG uptake was present at the middle of the nucleus close to its lateral boundary. While moving rostrad we observed its position to shift from the lateral to the ventral border of the nucleus. In the absence of CO segments, the somatotopic representation of the whiskerpad could not be ascertained. However, the spatially restricted zone of increased DG uptake points to a discrete representation of whisker follicles in this subnucleus as well, even in the absence of a visible map. Our observation is supported by the report of Bates and Killackey[4], who saw, in horizontal sections of the rat brainstem, 'rostrocaudal columns of dense SDH staining in the ventral portion of the nucleus'. It remains unclear, why neither these authors nor Ma[40] and ourselves saw such columns in transverse sections through So.

In Np, one area of stimulus-dependent DG uptake was found. It spanned CO segments across all five rows at the ventral and lateral boundary of the nucleus. The location of the area in the nucleus agrees with the morphological whisker map: the more peripheral CO segments that represent the more caudal whiskers, are situated near the ventrolateral limit of the nucleus[20]. The lack of precision of DG uptake of individual whisker representations in Np is probably due to limitations of the method, such as the traveling range of the beta rays (reported to be 20 μm) and the diffusion of the tracer.

In VB, the pattern of CO segments observed in our material matched the one in SDH-stained sections of the rat and mouse thalamus as documented by Belford and Killackey[5]. Comparing CO- with adjacent Nissl-stained sections, we agree with the conclusion of others[5,20,37,80], that the segments of high enzymatic activity coincide with the hollows of barreloids[64]. In adjacent coronal sections through VB, we found in mice from P7 to P11 one area of stimulus-dependent DG uptake covering up to five neighboring barreloids. The area of stimulus-dependent DG uptake was located at the lateral boundary of VB. This observation agrees with the functional[69] and morphological[64] maps reported earlier. The coronal sections were of no use to allocate individual barreloids to particular whiskers. The fact that we found more barreloids with high DG uptake than whiskers stimulated, may be related to the widespread distribution of neural activation in Np.

In BC, reconstructions of the barrelfield were based on Nissl-stained tangential sections. The superposition of these reconstructions on autoradiograms showed that, already at P10, stimulus-dependent DG uptake was restricted to the barrels whose whiskers were stimulated.

In summary, in Sc, Si, Np and BC, whisker follicles are represented in metabolic maps which are in harmony with the topography of follicle representations shown by histological methods. In VB, of which we had only coronal sections at our disposal, we could not establish such a relationship. Only brains cut in a near-horizontal plane[64] would allow comparison of metabolic and morphological maps.

III. Relationship between areas of increased DG uptake and areas of representations of whisker follicles

In brainstem as well as in cortex, we observed that, at the onset of stimulus-dependent DG uptake, the area of uptake covered more CO segments or barrels than the number of deflected whiskers. This may have been due to stimulation of follicles neighboring the deflected follicles as a consequence of closer mutual proximity of the whiskers and softness of the muzzle tissue in the young animals. If true, one would expect that using higher stimulus strength would lead to an increased area of stimulus-dependent DG uptake. However, the size of activated areas was found *not* to be related to stimulus strength as observed in mice stimulated at P4 or P7. Other possible mechanisms explaining the initial mismatch are discussed below.

a. Subcortical stations

In Sc and Si of animals of up to P11, the large and the small area of stimulus-dependent DG uptake were larger than the CO segments representing whisker follicles C1–3 and E1, respectively. The greatest mismatch occurred at P7–P11. At P13, the areas were almost confined to the appropriate segments.

The initial mismatch may be partially due to a dislocation of the tracer during the processing of the tissue. In the small and more watery brainstems of young mice, such a dislocation may have more serious consequences than in those of adults; moreover, the risk of melting the frozen tissue when blocking the brain is higher in small than in large specimens. On the other hand, the comparison between areas of increased DG uptake and the CO segments was made at an increased magnification at which CO boundaries could be drawn. For this we reproduced autoradiograms to

scale using hard paper, which may have led to an underestimation of the size of areas of stimulus-dependent DG uptake.

The greatest relative enlargement of the areas of stimulus-dependent DG uptake coincides with the highest magnitude of uptake. This may suggest a transient exuberant projection of fibers spreading into neighboring representations accompanied by hyperinnervation of the representations themselves. This is in harmony with the observation that trigeminal afferents in the rat have widespread arborizations in the nuclei of termination before P7[14]. Unfortunately, so far there is no report on the development of the ascending projections to VB. As an alternative or complementary process we propose the establishment of inhibitory corticofugal circuits (see Section IV).

b. Barrel cortex

At the onset of stimulus-dependent DG uptake in barrel cortex (P7), DG uptake was also increased in barrels whose whisker follicles had not been stimulated. The tangential extent of the area of stimulus-dependent DG uptake was independent from the strength of stimulation. This contrasts with our findings at P10 where, at low strength routine stimulation, stimulus-dependent DG uptake formed columns reaching from layer II to white matter, while in layer IV the uptake was confined to the barrels corresponding to the deflected whisker(s). DG uptake in the columns of barrels C1–3 was highlighted by a rim of depressed DG uptake which surrounds the excited barrels, and which was more accentuated in the D than in the B barrels. Such a rim was also observed after stimulation in adult mice of whisker B2 (see Fig. 5 in ref. 43 column a, bottom) or of whisker C3 (see Fig. 3D in ref. 9).

The restriction of the area of stimulus-dependent DG uptake to the barrels whose whiskers were stimulated, shown to occur between P7 and P10, may be explained by the development of two mechanisms operating in the adult forebrain.

The development of one circuit is related to inhibitory interneurons within the barrel cortex. These neurons may be responsible for the suppression of neuronal activity in the zone surrounding the activated cortical column; see below.

Alternatively, the restriction may result from the maturation of the connections from the barrel cortex to the reticular nucleus of the thalamus[24], and/or between that nucleus and VB. As a result of the development of this pathway, pyramidal cells in layer VI of the stimulated cortical column may activate neurons of the reticular nucleus, known to be GABAergic[17]. This activation, in turn, would result in the suppression of neuronal activity of neurons in VB that surround the stimulated barreloids. The restriction of the area of stimulus-dependent DG uptake to the barrels whose whiskers were stimulated, was accompanied by the appearance of a rim of decreased DG uptake surrounding the stimulated area. We interpret this decrease to be a sign of inhibition, in analogy to the observations of Webster et al.[71] in the cat auditory pathway, where it was shown that the electrophysiologically identified 'inhibitory side band' in the inferior colliculus was characterized by a level of DG uptake lower than neighboring unstimulated zones.

The observed shrinkage of areas of stimulus-dependent DG uptake during cortical maturation is in harmony with electrophysiological data from units in layer IV of the rat somatosensory cortex[1]. At P5 or 6, units were found which could be driven by 6 to 12 separately deflected whiskers. In the adult, and under identical conditions, a mean of two whiskers was found. In the same study, units were recorded in SI which responded to indentation of skin of the hind limb. In young rats, these neurons responded purely with excitation, whereas in adults the area of skin that elicited an excitatory response was surrounded by a field from which the cortical unit was inhibited. Mountcastle[49] had been the first to demonstrate what he termed 'surround inhibition' in somatosensory cortex of the adult cat by recording single- and multi-unit responses to skin indentation. Armstrong-James[1], in analogy to his observations on the hind limb representation, assumed that in the developing barrel cortex the shrinkage of receptive fields of neurons responding to whisker deflection, was based on an increase of surround inhibition. In our experiments an increase of surround inhibition during development may well have been the cause for the restriction of stimulus-dependent DG uptake to the barrels whose whiskers were stimulated. The zones of stimulus-dependent inhibition, centered around the stimulated barrels C1–3 and E1, are superimposed in the barrels of row D. This may have caused DG-uptake in the D barrels to be lower than in the barrels of row B.

Interestingly, the restriction of the area of stimulus-dependent DG uptake so as to match the morphological representations of the stimulated follicles first occurs in barrel cortex and manifests itself only three days later in the brainstem. This sequence of events suggests a role of the cortex in the refinement of the topography of the metabolic whisker representations in the brainstem. In adult mice projections originating from one cortical barrel column terminate in the corresponding whisker representation in the brainstem[73].

However, the development of these projections is not known.

IV. The increase and the decline of stimulus-dependent DG uptake

In the experiments with mice at P4 and older, stimulus-dependent DG uptake in the subcortical relays of the whisker-to-barrel pathway increased to a maximum between P7 and P10, then dropped considerably. This decline in neural activity may be due to inhibition mediated by corticofugal connections. It would be interesting to confirm whether, indeed, corticofugal projections are laid down and become functional during this period. Single- and multi-unit recordings in adult cats showed that cortical inputs to the sensory trigeminal brainstem nuclei[59] can facilitate or inhibit the spiking activity of ascending projection neurons[19]. Concerning the adult whisker-to-barrel pathway, a cortically mediated inhibition in the brainstem nuclei may well dominate a cortically mediated excitation. Cortically mediated inhibition in this pathway was reported to exist in the rat[79]. In cat, autoradiography of anterogradely transported proteins after intracortical injection of tritiated amino acids showed that corticotrigeminal axons invade the trigeminal sensory nuclei towards the end of the first postnatal week[63]. An anterograde tracer study attempting to elucidate the development of the corticotrigeminal projection in mice would be most interesting, as would be a DG study of the sensory trigeminal nuclei in adult mice whose barrel cortex is inactivated by either an acute lesion or cooling, in order to test whether or not the corticofugal connections play the inhibitory role we postulate here and their role in the reduction in area of DG uptake as proposed in section III of the Discussion.

In conclusion, the present study showed that, early in postnatal development of the mouse, functional whisker maps in the whisker-to-barrel pathway not only are somatotopically organized, but also are laid down sequentially from brainstem to cortex. Future work will be directed to the question whether the delivery of peripheral stimuli during development may influence temporal, structural and/or functional aspects of the development of the organization of a sensory system.

Acknowledgements. We thank S. Daldoss, E. Bernardi, D. Stucki and E. Brun for photography; R. Kraftsik and N. Jeanprètre, for assistance with statistical problems; G.M. Innocenti and members of the Lausanne Barrel Club for helpful comments; the family Fritschy for hospitality during one of the critical phases in the preparation of the final manuscript. Support: Swiss National Science Foundation Grants 3.238, 3.158 and 31-30932 to H.V.d.L., and fellowships by the 'Studienstiftung des deutschen Volkes' and the 'Deutsche Forschungsgemeinschaft' to P.M., who submitted this study to the Johann Wolfgang Goethe Universität, Frankfurt a.M., Germany, as partial fulfillment of the requirements for the Ph.D.-degree.

REFERENCES

1 Armstrong-James, M., The functional status and columnar organization of single cells responding to cutaneous stimulation in neonatal rat somatosensory cortex S1, *J. Physiol.*, 256 (1975) 501–538.
2 Arvidsson, J., Somatotopic organization of vibrissae afferents in the trigeminal sensory nuclei of the rat studied by transganglionic transport of HRP, *J. Comp. Neurol.*, 211 (1982) 84–92.
3 Astic, L. and Saucier, D., Ontogenesis of the functional activity of rat olfactory bulb: autoradiographic study with the 2-deoxyglucose method, *Dev. Brain Res.*, 2 (1982) 243–256.
4 Bates, C.A. and Killackey, H.P., The organization of the neonatal rat's brainstem trigeminal complex and its role in the formation of central trigeminal patterns, *J. Comp. Neurol.*, 240 (1985) 265–287.
5 Belford, G.R. and Killackey, H.P., Vibrissae representation in subcortical trigeminal centers of the neonatal rat, *J. Comp. Neurol.*, 183 (1979) 305–322.
6 Bernardo, K.L. and Woolsey, T.A., Axonal trajectories between mouse somatosensory thalamus and cortex, *J. Comp. Neurol.*, 258 (1987) 542–564.
7 Blue, M.E. and Molliver, M.E., Serotonin influences barrel formation in developing somatosensory cortex of the rat, *Soc. Neurosci. Abstr.*, 15 (1989) 419 (abstract).
8 Chiaia, N.L., Fish, S.E., Bauer, W.R., Bennett-Clarke, C.A., Rhoades, R.W., Postnatal blockade of cortical activity by tetrodotoxin does not disrupt the formation of vibrissa-related patterns in the rat's somatosensory cortex, *Dev. Brain Res.*, 66 (1992) 244–250.
9 Chmielowska, J., Kossut, M. and Chmielowski, M., Single vibrissal cortical column in the mouse labeled with 2-deoxyglucose, *Exp. Brain Res.*, 63 (1986) 607–619.
10 Collins, R.C., Use of cortical circuits during focal penicillin seizures: an autoradiographic study with [14C]deoxyglucose, *Brain Res.*, 150 (1978) 487–501.
11 Cooper, N.G.F. and Steindler, D.A., Lectins demarcate the barrel subfield in the somatosensory cortex of the early postnatal mouse, *J. Comp. Neurol.*, 249 (1986) 157–169.
12 Corthésy, M.-E., Rao, S.B., Welker, E., Dörfl, J., Van der Loos, H. and Hornung, J.-P., Plasticity occurs in the spinal trigeminal nucleus of the adult mouse upon partial peripheral deprivation, *Soc. Neurosci. Abstr.*, 17 (1991) 291 (abstract).
13 Cremer, J.E., Substrate utilization and brain development, *J. Cereb. Blood Flow Metabol.*, 2 (1982) 394–407.
14 Crissman, R.S., Parsons, L.L., Chiaia, N.L. and Rhoades, R.W., The primary afferent innervation of the trigeminal brainstem complex of fetal rats as demonstrated by anterograde transport of DI-I, *Soc. Neurosci. Abstr.*, 15 (1989) 873 (abstract).
15 Curtis, C.G., Cross, S.A.M., McCulloch, R.J. and Powell, G.M., *Whole-body autoradiography*, Academic Press, London, 1981, pp. 38–39.
16 Dahlquist, G. and Persson, B., The rate of cerebral utilization of glucose, ketone bodies, and oxygen: a comparative in vivo study of infant and adult rats, *Pediat. Res.*, 10 (1976) 910–917.
17 De Biasi, S., Frassoni, C. and Spreafico, R., Immunoreactivity in the thalamic reticular nucleus of the rat, *Brain Res.*, 399 (1986) 143–147.
18 Deuel, R.K., Yue, G.M., Sherman, W.R., Schickner, D.J. and Ackerman, J.J.H., Monitoring the time course of cerebral deoxyglucose metabolism by ^{31}P nuclear magnetic resonance spectroscopy, *Science*, 228 (1985) 1329–1331.
19 Dubner, R. and Sessle, B.J., Presynaptic modification of corticofugal fibers participating in a feedback loop between trigeminal brainstem nuclei and sensorimotor cortex. In R. Dubner and Y. Kawamura (Eds.), *Oral-Facial Sensory Motor Mechanisms*, Appleton-Century-Crofts Educational Division, Meredith Cor., New York, 1971, pp. 299–313.

20 Durham, D. and Woolsey, T.A., Effects of neonatal whisker lesions on mouse central trigeminal pathway, *J. Comp. Neurol.*, 223 (1984) 424–447.

21 Erzurumlu, R.S. and Killackey, H.P., Development of order in the rat trigeminal system, *J. Comp. Neurol.*, 213 (1983) 365–380.

22 Hawkins, R.A. and Miller, A.L., Loss of radioactive 2-deoxy-D-glucose-6-phosphate from brains of conscious rats: implications for quantitative autoradiographic determination of regional glucose utilization, *Neuroscience*, 3 (1978) 251–258.

23 Henderson, T.A., Woolsey, T.A. and Jacquin, M.F., Infraorbital nerve blockade from birth does not disrupt central trigeminal pattern formation in the rat, *Dev. Brain Res.*, 66 (1992) 146–152.

24 Hoogland, P.V., Welker, E. and Van der Loos, H., Organization of the projections from barrel cortex to thalamus in mice studied with *Phaseolus vulgaris*-leucoagglutinin and HRP, *Exp. Brain Res.*, 68 (1987) 73–87.

25 Huang, M. and Veech, R.L., The quantitative determination of the in vivo dephosphorylation of glucose-6-phosphate in rat brain, *J. Biol. Chem.*, 257 (1982) 11358–11363.

26 Jacquin, M.F., Renehan, W.E., Mooney, R.D. and Rhoades, R.W., Structure-function relationships in rat medullary and cervical dorsal horns. I. Trigeminal afferents, *J. Neurophysiol.*, 55 (1986) 1153–1186.

27 Jacquin, M.F., Woerner, D., Szczepanik, A.M., Riecker, V., Mooney, R.D. and Rhoades, R.W., Structure-function relationships in rat brainstem subnucleus interpolaris. I. Vibrissae primary afferents, *J. Comp. Neurol.*, 243 (1986) 266–279.

28 Jeanmonod, D., Rice, F.L. and Van der Loos, H., Mouse somatosensory cortex: alterations in the barrelfield following receptor injury at different early postnatal ages, *Neuroscience*, 6 (1981) 1503–1535.

29 Jensen, K.F., The development of the vibrissae related neocortical afferents to somatosensory cortex of the rat, *Soc. Neurosci. Abstr.*, 13 (1987) 77 (abstract).

30 Jensen, K.F. and Killackey, H.P., Terminal arbors projecting to the somatosensory cortex of the adult rat. I. The normal morphology of specific thalamocortical afferents, *J. Neurosci.*, 7 (1987) 3529–3543.

31 Jhaveri, S., Erzurumlu, R.S. and Crossin, K., Barrel construction in rodent neocortex: role of thalamic afferents versus extracellular matrix molecules, *Proc. Natl. Acad. Sci. USA*, 88 (1991) 4489–4493.

32 Kadekaro, M., Crane, A.M. and Sokoloff, L., Differential effects of electrical stimulation of sciatic nerve on metabolic activity in spinal cord and dorsal root ganglion in the rat, Proc. Natl. Acad. Sci. USA, 82 (1985) 6010–6013.

33 Kadekaro, M., Vance, W.H., Terrell, M.L., Gary Jr., H., Eisenberg, H.M. and Sokoloff, L., Effects of antidromic stimulation of the ventral root on glucose utilization in the ventral horn of the spinal cord in the rat, *Proc. Natl. Acad. Sci. USA*, 84 (1987) 5492–5495.

34 Killackey, H.P. and Belford, G.R., The formation of afferent patterns in the somatosensory cortex of the neonatal rat, *J. Comp. Neurol.*, 183 (1979) 285–304.

35 Kloss, G., Kellner, H.-M. and Kötter, Chr., Vakuum-Kontakt-Methode bei der Makroautoradiographie, *Z. Naturforsch.*, 28 (1973) 468.

36 Kossut, M. and Hand, P., The development of the vibrissal cortical column: a 2-deoxyglucose study in the rat, *Neurosci. Lett.*, 46 (1984) 1–6.

37 Land, P.W. and Simons, D.J., Metabolic and structural correlates of the vibrissae representation in the thalamus of the adult rat, *Neurosci. Lett.*, 60 (1985) 319–324.

38 Land, P.W. and Simons, D.J., Cytochrome oxidase staining in the rat SmI barrel cortex, *J. Comp. Neurol.*, 238 (1985) 225–235.

39 Ma, P.M., The barrelettes – architectonic vibrissal representations in the brainstem trigeminal complex of the mouse. I. Normal structural organization, *J. Comp. Neurol.*, 309 (1991) 161–199.

40 Ma, P.M., Barrelettes – architectonic vibrissal representations in the brainstem trigeminal complex of the mouse. II. Normal post-natal development, *J. Comp. Neurol.*, 327 (1993) 376–397.

41 Ma, P.M. and Woolsey, T.A., Cytoarchitectonic correlates of the vibrissae in the medullary trigeminal complex of the mouse, *Brain Res.*, 306 (1984) 374–379.

42 McCasland, J.S., Carvell, G.E., Simons, D.J. and Woolsey, T.A., Functional asymmetries in the rodent barrel cortex, *Somatosens. Motor Res.*, 8 (1991) 111–116.

43 Melzer, P., Van der Loos, H., Dörfl, J., Welker, E., Robert, P., Emery, D. and Berini, J.-Ch., A magnetic device to stimulate selected whiskers of freely moving or restrained small rodents; its application in a deoxyglucose study, *Brain Res.*, 348 (1985) 229–240.

44 Melzer, P., Welker, E., Dörfl, J. and Van der Loos, H., The onset of response to whisker stimulation in mouse barrelfield (BF), a deoxyglucose (DG) and cytochrome oxidase (CO) study, *Experientia*, 40 (1984) 631 (abstract).

45 Melzer, P., Welker, E., Dörfl, J. and Van der Loos, H., Metabolic signs of early cortical response to whisker stimulation in mice, a deoxyglucose (DG) and cytochrome oxidase (CO) study, *Neurosci. Lett.*, Suppl. 18 (1984) S299 (abstract).

46 Melzer, P., Welker, E., Dörfl, J. and Van der Loos, H., The dependence of stimulus-dependent responses in the barrelfield (BF) of the mouse on the intensity of vibrissa stimulation: a deoxyglucose (DG) study, *Neurosci. Lett.*, Suppl. 22 (1985) S424 (abstract).

47 Melzer, P., Welker, E., Dörfl, J. and Van der Loos, H., Development of order in the whisker-to-barrel pathway of the mouse: neuronal metabolic responses to whisker stimulation, *Soc. Neurosci. Abstr.*, 12 (1986) 953 (abstract).

48 Melzer, P., Welker, E., Dörfl, J. and Van der Loos, H., Whisker stimulation increases ketone body (KB) metabolism in infant mouse trigeminal subnuclei caudalis (SC) and interpolaris (SI), *Experientia*, 43 (1987) 671 (abstract).

49 Mountcastle, V.B., Modality and topographical properties of single neurons of cat's somatic sensory cortex, *J. Neurophysiol.*, 20 (1957) 408–434.

50 Nelson, T., Lucignani, G., Atlas, S., Crane, A.M., Diene, G.A. and Sokoloff, L., Reexamination of glucose-6-phosphatase activity in the brain in vivo: no evidence for a futile cycle, *Science*, 229 (1985) 60–62.

51 Rhoades, R.W., Bennet-Clarke, C.A., Chiaia, N.L., White, F.A., MacDonald, G.J., Haring, G.J. and Jacquin, M.F., Development and lesion induced reorganization of the cortical representation of the rat's body surface as revealed by immunohistochemistry for serotonin, *J. Comp. Neurol.*, 293 (1990) 190–207.

52 Rice, F.L. and Anders, D., A small guillotine to prepare brains for sectioning in defined, odd planes, *Neurosci. Lett.*, 6 (1977) 157–163.

53 Rice, F.L. and Van der Loos, H., Development of the barrels and the barrel field in the somatosensory cortex of the mouse, *J. Comp. Neurol.*, 171 (1977) 545–560.

54 Ryan, A.F., Woolf, N.K. and Sharp, F.R., Functional ontogeny in the central auditory pathway of the mongolian gerbil, *Exp. Brain Res.*, 47 (1982) 428–436.

55 Sacks, W., Sacks, S. and Fleischer, A.A., A comparison of the cerebral uptake and metabolism of labelled glucose and deoxyglucose in vivo in rats, *Neurochem. Res.*, 8 (1983) 661–685.

56 SAS Institute Inc., *SAS/STAT User's guide*, SAS Institute Inc., Cary, NC, 1990.

57 Schwartz, W.J., Smith, C.B., Davidson, L., Savaki, H., Sokoloff, L., Mata, M., Fink, D.J and Gainer, H., Metabolic mapping of functional activity in the hypothalamo-neurohypophysial system of the rat, *Science*, 205 (1979) 723–725.

58 Senft, S.S. and Woolsey, T.A., Growth of thalamic afferents into mouse barrel cortex, *Cereb. Cortex*, 1 (1991) 308–335.

59 Sessle, B.J. and Dubner, R., Presynaptic depolarization and hyperpolarization of trigeminal primary and thalamic afferents. In R. Dubner and Y. Kawamura (Eds.), *Oral-Facial Sensory and Motor Mechanisms*, Appleton-Century-Crofts Educational Division, Meredith Cor., New York, 1971, pp. 279–297.

60 Simons, D.J., Temporal and spatial integration in the rat SI vibrissa cortex, *J. Neurophysiol.*, 54 (1985) 615–635.

61 Sokoloff, L., The ^{14}C deoxyglucose method: four years later, *Acta Neurol. Scand.*, 60 Suppl., 72 (1979) 640–649.
62 Sokoloff, L., Reivich, M., Kennedy, C., Des Rosier, M.H., Patlak, C.S., Pettigrew, K.D., Sakurada, O. and Shinohara, M., The ^{14}C deoxyglucose method for the measurement of local cerebral glucose utilization: theory, procedure, and normal values in the conscious and anesthetized albino rat, *J. Neurochem.*, 28 (1977) 897–916.
63 Tolbert, D.L., Dunn Jr., R.C. and Vogler, G.A., The postnatal development of corticotrigeminal projections in the cat, *J. Comp. Neurol.*, 228 (1984) 478–490.
64 Van der Loos, H., Barreloids in mouse somatosensory thalamus, *Neurosci. Lett.*, 2 (1976) 1–6.
65 Van der Loos, H., Dörfl, J. and Welker, E., Variation in pattern of mystacial vibrissae in mice. A quantitative study of ICR stock and several inbred strains, *J. Hered.*, 75 (1984) 326–336.
66 Van der Loos, H. and Woolsey, T.A., Somatosensory cortex: structural alterations following early injury to sense organs, *Science*, 179 (1973) 395–398.
67 Verley, R. and Axelrad, H., Postnatal ontogenesis of potentials elicited in the cerebral cortex by afferent stimulation, *Neurosci. Lett.*, 1 (1975) 99–104.
68 Verley, R. and Gaillard, P., Postnatal ontogenesis of potentials elicited in the barrelfield of mice by stimulation of the maxillary nerve, *Neurosci. Lett.*, 10 (1978) 121–127.
69 Waite, P.M.E., Somatotopic organization of vibrissal responses in the ventrobasal complex of the rat thalamus, *J. Physiol.*, 228 (1973) 527–540.
70 Waite, P.M.E., Normal nerve fibers in the barrel region of developing and adult mouse cortex, *J. Comp. Neurol.*, 173 (1977) 165–174.
71 Webster, W.R., Servière, J., Martin, R. and Brown, M., Uncrossed and crossed inhibition in the inferior colliculus of the cat: a combined 2-deoxyglucose and electrophysiological study, *J. Neurosci.*, 5 (1985) 1820–1832.
72 Webster, W.R., Servière, J., Martin, R. and Hartley, E., Tonotopic bands produced by tones commenced long after 2-deoxyglucose injection, *Neurosci. Lett.*, 40 (1983) 281–286.
73 Welker, E., Hoogland, P.V. and Van der Loos, H., Organization of feedback and feedforward projections of the barrel cortex: a PHA-L study in the mouse, *Exp. Brain Res.*, 73 (1988) 411–435.
74 White, E.L., Identified neurons in mouse SmI cortex which are postsynaptic to thalamocortical axon terminals: a combined Golgi-electron microscopic and degeneration study, *J. Comp. Neurol.*, 181 (1978) 627–662.
75 Wong-Riley, M.T.T., Changes in the visual system of monocularly sutured or enucleated cats demonstrable with cytochrome oxidase histochemistry, *Brain Res.*, 171 (1979) 11–28.
76 Wong-Riley, M.T.T. and Welt, C., Histochemical changes in cytochrome oxidase of cortical barrels after vibrissal removal in neonatal and adult mice, *Proc. Nat. Acad. Sci. USA*, 77 (1980) 2333–2337.
77 Woolsey, T.A. and Van der Loos, H., The structural organization of layer IV in the somatosensory region (SI) of mouse cerebral cortex. The description of a cortical field composed of discrete cytoarchitectonic units, *Brain Res.*, 17 (1970) 205–242.
78 Woolsey, T.A. and Wann, J.R., Areal changes in mouse cortical barrels following vibrissal damage at different postnatal ages, *J. Comp. Neurol.*, 170 (1976) 53–66.
79 Woolston, D.C., La Londe, J. and Gibson, J.M., Corticofugal influences in the rat on responses of neurons in the trigeminal nucleus interpolaris to mechanical stimulation, *Neurosci. Lett.*, 36 (1983) 43–48.
80 Yamakado, M., Postnatal development of barreloid neuropils in the ventrobasal complex of mouse thalamus: a histochemical study for cytochrome oxidase, *Brain Nerve*, 37 (1985) 497–506.
81 Yarris, L.M., Chiaia, N.L., Bennett-Clarke, C.A., Jacquin, M.F., Haring, J.H., Macdonald, G.J., and Rhoades, R.W., Serotonin immunoreactive fibers yield a complete map of the body surface in somatosensory cortex of perinatal rats, *Soc. Neurosci. Abstr.*, 15 (1989) 874 (abstract).